

BIBLIOGRAPHY

Edited by Z. Kopal, M. Moutsoulas, and J. W. Salisbury

1. Motion of the Moon in Space and Dynamics of the Earth-Moon System, Lunar Astronautics

Baumgartner, W. S. and Easterling, M. F.: 'A World-Wide Lunar Radar Time Synchronization System', AGARD Advanced Navigational Tech., Jan. 1970, pp. 143-162.

A system is described which is capable of synchronizing clocks at remote locations with a master clock to within a few microseconds by means of radar reflections from the Moon for the Deep Space Network. The needs of the Deep Space Network for time synchronization are described, several possible methods of synchronizing are compared, and the factors favoring the radar method are given. The method by which a range gated radar may be used to obtain precise time synchronization via a diffuse target is described and a theory for calculating the performance of such a radar is developed. An analysis using this theory shows that a radar with quite modest capability will produce a detectable return signal. Because it was desired to synchronize many remote clocks to one master clock, the design was constrained to make the radar receiver, which is located with the remote clock, as simple as possible. It proved feasible to use a fixed tuned receiver with a four-foot antenna and inherently unattended operation. Test results and operating experience are presented and analyzed.

Breland, G. W.: 'Lunar Far Side Communications Coverage and Visibility Analysis for Satellite Relay Systems', NASA Contractor's Report-108327.

The coverage and visibility analysis for lunar orbiting communications satellites is documented. This study is a part of an overall system study for a lunar far side satellite relay communications system. The study program encompasses three tasks: (1) communications system parametric analysis; (2) trajectory and vehicle considerations; and (3) survey of applicable technology. The communications system parametric analysis is based upon a mathematical model of a satellite communications system. Requirements for relay satellite system parameters such as effective radiated power, noise, temperature, etc., are being investigated for three types of lunar terminal: current Apollo systems, improved Apollo systems, and new communications terminals. Trajectory and vehicle considerations include performance, trajectory, and guidance analysis which encompass, but are not limited to, the following major items: Delta V requirements for entering selected lunar orbits, payload capabilities of candidate launch vehicles, perturbative effects on selected lunar orbits, propulsion requirements for orbit stabilization, and methods of deploying multiple satellites from a single launch vehicle. The survey of applicable communications satellite technology is directed toward an assessment of the current state-of-the-art in the major system such as tracking antenna design, RF power capabilities, and reliability, etc.

Breland, G. W., Lorio, L. A., Miller, J. C., Penzo, P. A., and Perron, D. R.: 'Lunar Far Side Communications Analysis for Satellite Relay Systems', NASA-Contractor's Report-108412.

Orbiting lunar relay satellites are considered for manned landing missions on the lunar far side. Since full coverage of the lunar far side surface is not possible from an equatorial orbit, a system of polar orbiting relay satellites is proposed. For continuous coverage of the entire lunar sphere, the minimum

network of relay satellites is composed of three sets of three orbiting satellites, equally spaced in circular orbits. Since the most attractive possibility for partial coverage is a network of three equally spaced satellites in circular polar orbit, it is proposed that such a system be established as an interim step in providing full coverage with the nine satellite system. The study indicates that as many as three satellites weighing approximately 2000 pounds each can be placed in lunar orbit with a single booster presently available. The various antenna and power configurations for the proposed satellite network are discussed.

Cameron, A. G. W.: 'Formation of the Earth-Moon System', *EOS* **51**, 350.

The formation of the solar system is now thought to have been a part of the process of a collapse of an interstellar cloud. In a recent analysis of the structure of the resulting gaseous disk, the author concluded that the inner part would be unstable against convection. Von Weizsacker, Ter Haar, and the author have all concluded that such a turbulent, gaseous disk will dissipate in a time of order 10^8 years. The inner planets must form in this time. For the Earth, this implies temperatures near 10^4 K, with an outer envelope consisting mainly of magnesium silicates and their decomposition products and extending to several Earth radii. With the present angular momentum of the Earth-Moon system, the atmosphere will be in orbital motion in the equatorial plane beyond three Earth radii, and from this atmosphere the Moon can collect deficient in iron and the more volatile elements. Initial lunar interior temperatures will be near 10^3 K. Subsequently the Earth can collect an extra ten percent of cold bodies which bring in volatile elements and tilt the spin axis away from the lunar orbital plane. (Abstract of a paper presented at the April 1970 meeting of the American Geophysical Union.)

Deprit, A., Henrard, J., and Rom, A.: 'Analytical Lunar Ephemeris: 1. Definition of the Main Problem', Boeing Scientific Research Labs. Document D1-82-0936.

A new set of phase variables is proposed and justified to develop automatically by computer the solar terms in Lunar Theory.

The dependence of the perturbation function on the mass ratio Moon/(Earth + Moon) is completely elucidated. A recursive procedure is proposed to develop that function so as to keep explicit all its d'Alembert characteristics.

The perturbation series obtained by computer is compared with Delaunay's development.

Edelbaum, T. N.: 'Libration Point Rendezvous', NASA-Contractor's Report-86337; Rept-70-12.

A study of the flight mechanics and mass requirements for one-shot lunar missions were made utilizing rendezvous at the libration points in front of, and behind, the Moon. The flight mechanics studies were carried out using the restricted problem of three-bodies. It was found that the lowest ΔV requirement to reach either libration point was to go to the L_2 point behind the Moon via a powered lunar swingby. It was also found that every point on the lunar surface is directly accessible from the L_2 point, for transfer times greater than about 59 hours. The mass calculations were carried out assuming advanced cryogenic propellants in all stages. For such propellants, the least mass in Earth orbit for rendezvous at the L_2 point was determined. The mass requirement was found to be smaller than that for the standard lunar orbit rendezvous mode. Rendezvous at either the L_2 point, or in a Halo Orbit about the L_2 point, would also have operational advantages, including access to all points on the Moon and an infinite rendezvous launch window.

Egorov, V. A.: 'Three-dimensional Lunar Trajectories' (Transl. into English of the book *Prostranstvennaya Zadacha Dostizheniya Lunny*), NASA-Technical Translation-F-504.

Hall, J. R.: 'Tracking and Data system Support for Lunar Orbiter', NASA-Contractor's Report-109875; JPL-Technical Memorandum-33-450.

Hurt, G. J., Jr., Bergeron, H. P., and Adams, J. J.: 'An Evaluation of Two Guidance Schemes for a Manned Lunar Landing', NASA-Technical Note-D-5817; L-6761.

A fixed-base simulation of a lunar descent was performed. The simulation, using instruments only, was conducted to compare two vehicle attitude programs: a single pitch-angle change and a multiple pitch-angle change. The comparison was made to determine a pilot's ability to complete a lunar descent from a 50000-foot (15240 meters) circular orbit to a hover altitude of approximately 1000 feet (305 meters) after a malfunction had forced the pilot to take control. System failures which would have caused a disaster if the pilot had not assumed control were randomly introduced during the simulated descents. Either of the two letdown profiles could be handled by the pilots. The multiple pitch-angle profile appeared to afford the pilot greater chance for success than did the single pitch-angle profile.

Klock, B. L. and Scott, D. K.: 'Orientation of the FK4 Catalogue from Meridian Observations of the Moon', *Astron. J.* **75**, 851-856.

Equinox and equator point corrections to the FK4 catalogue system have been determined from six-inch transit circle observations of the Moon. Included in the discussion are corrections to orbital elements of the Moon. The validity of the use of the Moon to orient the fundamental reference system is questioned.

Krishnan, T.: 'The Effect of Receiver Bandwidth on Lunar Occultation Observations: Narrow Symmetric Passbands', NASA-Technical Note-D-5679.

A general expression is derived for the effect of receiver bandwidth on lunar occultation observations, the phenomenon being considered equivalent to diffraction at a straight edge. The expression is applied to derive the parameters defining effective beam due to bandwidth alone for five symmetrical and narrow passbands of common shape. It is shown that the half-power effective beamwidth in seconds of arc (for the mean Moon-Earth distance) varies between 6.2 and 7.2 times the square root of the absolute half-power bandwidth in wavelength expressed in meters. Sensitivity and beam shape evaluations indicate that in radio-astronomy applications, given a desired resolution, the single-tuned passband is optimal. When the beam shape is well behaved it is unnecessary to preconvolve the theoretical restoring function with a Gaussian, as is usually done.

Kutland, J. R. and Goodwin, C. H.: 'Analysis of a Communication Satellite for Lunar Far-side Exploration', NASA-Contractor's Report-110355.

The feasibility and conceptual design of a communication satellite which provides a real-time, two-way communications link between the Earth and a spacecraft located behind the Moon is presented. This satellite is capable of relaying colour television, voice, high-bit-rate telemetry data, and ranging code from the Command and Service Module and the Lunar Module during all phases of their mission. The 905-pound satellite has a useful lifetime of four years and is envisioned for launch in the 1973-74 period via a thrust augmented thor-delta vehicle. A lunar fly-by trajectory places the satellite behind the Moon in a bounded 3500 kilometer radius halo orbit about the Earth-Moon L_2 libration point. This halo orbit affords the satellite a continuous view of both the Earth and the entire lunar back side. However, due to the instability of this orbit, periodic orbit corrections are performed by a set of special thrusters.

Lukjanov, L.: 'On a Method of Determination of Earth and Moon Mass Ratio', *Astron. Zh.* **47** (1970), 894-901.

In order to correct the Earth and Moon mass ratio it is proposed to use observations of motion of an artificial satellite placed in the vicinity of triangular libration point of Earth-Moon system. The solution of the problem put forward by the author is based on the plane circle restricted problem of three bodies.

Martin, C. F. and Van Flandern, T. C.: 'Secular Changes in the Lunar Elements', *Science* **168**, 246–247.

Corrections to the adopted values for centennial rates of change of four elements of the lunar orbit, the location of the FK4 equinox, and the obliquity of the ecliptic are presented. They are derived from analyses of lunar occultations distributed over several centuries. Generally, these corrections help to resolve existing discrepancies between theory and observations.

Morrison, L. V.: 'On the Orientation of C. B. Watts' Charts of the Marginal Zone of the Moon', *Monthly Notices Roy. Astron. Soc.* **149**, 81–90.

It is shown, from an analysis of occultations of stars by the Moon, that limb profiles from Watts' charts accord better with observation when the tabular position angles of the charts are amended systematically by $-0^{\circ}.25 (\pm 0^{\circ}.01)$.

Poultney, S. K.: 'Report on December 1969 Performance and Calibration Trip to the Lunar Laser Ranging Station at McDonald Observatory', NASA-Contractor's Report-110208; Technical Report-70-075.

Performance of the detector package, Korad laser, receiver efficiency, and other portions of the laser ranging station during December 1969 is reported. A summary of start and stop line delay calibration is also included.

Poultney, S. K.: 'Report on January 1970 Performance and Calibration Trip to the Lunar Laser Ranging Station at McDonald Observatory', NASA-Contractor's Report-110205; Technical Report-70-087.

Performance of the detector package, Korad laser, receiver efficiency, and other portions of the laser ranging station is reported. A summary of start and stop line delay calibration is also included along with the results of the calibration procedure.

Poultney, S. K.: 'Time-Keeping for the Laser Ranging Experiment at McDonald Observatory', NASA-Contractor's Report 110207; Technical Report-70-021.

Poultney, S. K.: 'The Concept of the Time Interval Measurement and Control Circuitry for the Lunar Ranging Experiment: A History', NASA-Contractor's Report-110146; Technical Report-70-68.

The concept of the time interval measurement and control circuitry for the Lunar Ranging Experiment prior to January 1969 is recorded. The suggested components of the system are also given.

Poultney, S. K.: 'The Detector Package for the Laser Ranging Experiment at McDonald Observatory: Its Design, Performance and Operation', NASA-Contractor's Report-110217; Technical Report-957.

Rayner, J. D.: 'A Description of the Control Program for the Lunar Ranging Experiment', NASA-Contractor's Report-110210; Technical Report-70-064.

The lunar ranging ground station built around a Varian 620/i control computer is discussed. This arrangement gave operating flexibility, as well as providing computational capability. Three main computer functions were required: to control the firing of the laser and gate the return pulse, to calculate an approximate range from the data, and to record the raw data supplemented by calibration data on magnetic tape. The computer laser controls using two external control lines, one to fire the flash lamps and one to enable the Pockels cell are evaluated.

Singer, S. F.: 'The Early History of the Earth-Moon System', *EOS* 51, 350.

Using a frequency-dependent version of tidal theory in an elaborate orbit perturbation calculation, one derives for the early orbit of the Moon a parabola with low perigee and moderate inclination; i.e., direct rather than retrograde. This result suggests capture of the Moon, which is physically quite possible although of low probability. Tidal capture would produce extensive heating of the Earth's interior, followed by the immediate evolution of an atmosphere and hydrosphere. Heating of the Moon would produce some degree of differentiation and loss of volatiles. Evidence, both geological and lunar, appears to support the tidal capture hypothesis. (Abstract of a paper presented at the April 1970 meeting of the American Geophysical Union.)

Smith, T. J. and McGee, C. F.: 'Project Technical Report MSC/TRW Task KM-205: SLP OWS Control System Digital Simulation Requirements', NASA Contractor's Report 108363.

Equations and logic to be programmed for an all digital simulation of the AAP orbital workshop (OWS) pointing control system (PCS) and thrust attitude control system (TACS) are presented. The program was developed in a modular form such that the final software could be incorporated without disturbing the overall program structure. In many undefined areas, subroutines have been developed which anticipate the software to be incorporated in the onboard computer (on the basis of the physical principles involved and any available documentation). Changes to the simulation will be made as the software to be programmed in the onboard computer becomes finalized. A block diagram of the OWS attitude control systems (ACS) is shown. The portions of the OWS ACS which are modelled in this simulation include the CMG subsystem. The thrust attitude control system (TACS) jets, the pointing control system (PCS) and TACS software in the ATM digital computer, the star tracker, the vehicle rate gyros, and the acquisition Sun sensors.

Steggerda, D. A.: 'A Description of the Time Interval Measurement and Laser Control Circuitry for the Lunar Ranging Experiment', NASA-Contractor's Report 110140; Technical Report-70-049.

The laser control and time interval measurement circuits were combined with a detector package, a laser, and an astronomical telescope. This system is designed to measure the time of flight of a light pulse to a lunar retroreflector and back to an accuracy of 1 nanosecond with a precision of 100 picoseconds. The range is computed by adding an analog measurement of the time between the outgoing laser pulse and an initial frequency standard clock pulse. To prevent the system from measuring random photons, a window pulse is provided to activate the final time to pulse height converters. The lunar ephemeris, recorded on magnetic tape and read by a Varian data machines 620/i computer, is used to generate this window pulse.

TRW Systems Group: 'Apollo Mission-11, Trajectory Reconstruction and Post-flight Analysis; Volume 1', NASA Contractor's Report-108349.

The objective of the postflight analysis task was, in general, to generate trajectory parameters and data for the command and service modules and lunar module from S-IVB/CSM separation to the end of mission. As in the Apollo missions 9 and 10, a preliminary trajectory was generated from the best available RTCC vectors. The bulk of the post-flight analysis effort was then concentrated on reconstruction of the two periods of flight from LM/CSM undocking to LM touchdown (descent phase) and from LM ascent to LM/CSM docking (rendezvous). The RTCC vectors used to generate the preliminary NAT (NASA Apollo Trajectory) are summarized. Most of the lunar trajectories were generated using RTCC SS2 (inclination constrained) solution vectors rather than SS1 (no a priori) solution vectors. Unlike the Apollo-10 SS2 vectors which were constrained to the pre-LOI1, rev 18, and rev 29 planes, the Apollo 11 SS2 vectors were constrained on a rev to rev basis. Each SS2 vector contained two revs of data and was constrained to the SS1 solution plane of one of these two revs (exceptions existed at maneuvers). This technique prevented the accumulation of a large error in the out-of-plane component of position.

3. Shape and Gravitational Field of the Moon

Bullock, M. V. and Ferrari, A. J.: 'Orbit Determination for Lunar Parking Orbits using Time-varying Orbital Elements', NASA-Contractor's Report-110008; Technical Report-70-310-2.

A lunar orbit determination program (Osculating Lunar Elements Program – OLEP) has been developed that represents perturbed vehicle motion by time-varying orbital elements. The program estimates perturbing effects of non-central gravity anomalies, so the concept does not rely on any assumed lunar gravity model. Doppler tracking data from the lunar orbits of Lunar Orbiter-3, Apollo 8, 10, 11 and 12 missions have been processed, and the results are presented. The solutions obtained from these data show OLEP to be effective for use in lunar navigation and orbit prediction. A comparison between OLEP and one current standard technique shows OLEP propagation errors smaller by a factor of 2.5 or more. This concept shows potential for application to future Apollo missions and to deep space missions involving planets whose gravity fields are not well known.

Chuikova, N. A.: 'The Potential and Gravity Distribution on the Moon's Physical Surface', *Soviet Astron.* **13**, 878–880.

The distribution of potential and gravity over the Moon's physical surface can be established if the external gravitational potential of the Moon and the equation of its physical surface are known. The expansions of these distributions in spherical harmonics will contain harmonics of all the orders that occur in the expansions of the Moon's external potential and relief, together with all possible sums and differences of orders.

De Sabbata, V.: 'Lunar Mascons as Detector of Gravitational Waves from Pulsars', *Mem. Soc. Astron. Italiana* **41**, 65–67.

It is proposed to exploit the lunar mascons for the detection of gravitational radiation in the 1-Hz band, as that presumably emitted by pulsars. If the mascons give rise to a resonance effect in the seismic response, the possibility of the detection may be not too far from the existing instruments.

Gottlieb, P.: 'Estimation of Local Lunar Gravity Features', *Radio Sci.* **5**, 301–312.

A quantitative estimate of the gravity features on the near surface of the Moon has been obtained by iteratively constructing a mass density model to improve the agreement between actual Doppler tracking data from Lunar-Orbiter spacecraft and theoretical trajectory predictions. Thirty-three typical orbits (24 nearly polar and 9 nearly equatorial) were selected at 3 to 4 degree separations to cover most of the front side of the Moon. Each iterative stage consisted of placing masses near the lunar surface at locations indicated by the peak residual accelerations observed after fitting the data with the model constructed at the previous iteration.

Gottlieb, P., Muller, P. M., Sjogren, W. L., and Wollenhaupt, W. R.: 'Lunar Gravity over Large Craters from Apollo-12 Tracking Data,' *Science* **168**, 477–479.

The Doppler residuals from the Apollo-12 lunar module radio tracking data indicate large negative accelerations over the craters Ptolemaeus and Albategnius. The mass deficiencies required to produce these accelerations are approximately equivalent to the removal of the surface material to a depth of 1 kilometer over the entire area of these craters. Several other features of the gravity fine structure can also be correlated with topography.

Koch, K. R.: 'Lunar Shape and Gravity Field', *Photogrammetric Eng.* **36**, 375–380.

The positions of a metric camera in a spacecraft orbiting the Moon can be treated as unknown

parameters in a photogrammetric solution for establishing control points on the surface of the Moon. According to Newton's law of gravitation, however, the orbit of a spacecraft around the Moon, or the positions of the camera in a satellite on a photogrammetric mission, can be expressed by six orbital elements and the parameters of the lunar gravity field. Such a substitution of the camera positions not only reduces the number of unknown parameters but also provides an opportunity to gather information about the gravity field of the far side of the Moon where spacecraft cannot be tracked from the Earth.

Lorell, J. and Laing, P. A.: 'Compilation of Lunar Orbiter Tracking Data used for Long-term Selenu-
nology', NASA-Contractor's Report-109764; JPL-Technical Memorandum-33-419.

Tracking data from the five NASA lunar orbiters have been compressed into a set of normal points for use in studying the Moon's gravity field. This report makes these normal points available in tabulated form and gives auxiliary information concerning the lunar orbiter mission and tracking patterns pertinent to the use of the normal points.

Smith, D. E.: 'First-order Perturbations of an Orbit by a Mass Anomaly', NASA-Technical Memorandum-X-63921; X-550-70-85.

The first order short period perturbation of a satellite's position and the first order long period perturbations of the orbital elements by a mass anomaly are developed. It is shown that the maximum values of the secular and long period perturbations are about 300 and 80 meters in the along track and across track directions per revolution for a mascon of 0.00001 of the Moon's mass. In addition, short period perturbations were found with maximum amplitudes of about 15 meters in height, 40 meters in along track position, and 7 meters in the across track direction. The major assumptions made in the analysis were that the position of the mascon and the orbit of the spacecraft remained fixed in space over the integration period (one revolution). The former approximation can be justified because the Moon rotates very slowly and the later approximation is valid if the perturbations by all other forces are small, which is usually the case.

Wong, L., Downs, W., Buechler, G., Prislun, R., Sjogren, W., Muller, P., and Gottlieb, P.: 'Lunar Gravitational Model Derived from Doppler Observations,' *EOS* **51**, 267.

The near-side lunar gravitational field was inferred dynamically from Doppler observations of Lunar Orbiters 1 through 5 over short arcs of less than 75 minutes. The force model contains a surface distribution of disk masses. The magnitude of the masses were estimated simultaneously with the initial state vectors of all the arcs for a total of over 1500 simultaneously estimated parameters. A method for combining the near-side field with a low-degree spherical harmonics model to arrive at a composite field is described. This solution shows the original mascon areas and provides an improvement to the fit of the observations over a mascon model based on polar orbits alone. (Abstract of a paper presented at the April 1970 meeting of the American Geophysical Union.)

4. Internal Structure of the Moon

Cook, R. K.: 'A Model for the Moon's Seismic Reverberation', *EOS* **51**, 347.

The passage of an elastic wave through the body of the Moon is assumed to occur with continuous (in time) and homogeneous (in space) scattering and absorption. An impulse at a point on the surface produces a long (in time) reverberant seismic motion at another point. Parameters of the model are deduced from the observed rise and decay of reverberations at the Moon's surface. Another model considered is scattering by layers parallel to the surface, with scattering strength dependent on depth. (Abstract of a paper presented at the April 1970 meeting of the American Geophysical Union.)

Danes, Z. F.: 'Isostatic Processes on the Surface of the Moon,' *EOS* **51**, 210.

Large lunar craters undergo changes that can be explained if the interior of the Moon is assumed to be viscous. Craters of intermediate size change too, but at a slower rate; and small craters, of diameter of 17 km or less, stay virtually unchanged. This variation indicates that the Moon has a crust of about 4–7 km thickness and of 10^{25} poise viscosity, underlain by a 'mantle' of viscosity not greater than 10^{23} poise. Such a two-layer model can also account for the persistence of ridges of a width of 14 km or less, but absence of similar features of greater cross sectional dimensions. (Abstract of a paper presented at the March 1970 meeting of the American Geophysical Union.)

Pandit, B. I. and Tozer, D. C.: 'Anomalous Propagation of Elastic Energy Within the Moon,' *Nature* **226**, 335.

The authors point out a few observations that encourage the model of energy propagation as elastic waves over large distances represented as a diffusive process in a low loss elastic continuum.

Turcotte, D. L. and Oxburgh, E. R.: 'Lunar Convection,' *EOS* **51**, 348.

It has been shown that if the mean rate of lunar radioactive heat generation is similar to the terrestrial value, and if the Moon is relatively undifferentiated, thermal convection occurs with it. The ratio of surface area to volume is nearly four times greater for the Moon than for the Earth and consequently the cold and rigid outer layer (the lunar lithosphere) is much thicker (400 km). The lunar lithosphere is too thick to have fragmented into plates in relative motion as on Earth, and thus there is little lunar seismicity. On Earth convective motions extend to the surface (free-surface condition) and partial melting of mantle material occurs readily in zones of ascending flow through adiabatic pressure release. On the Moon convective motions are limited by the base of the lithosphere (fixed-surface condition) and the adiabatic pressure release may be too small for extensive melting. At an earlier stage in the Moon's history with a thinner lithosphere fusion could have occurred more readily. On Earth, mantle convection should occur with a pattern of unsteady rolls; on the Moon an annular pattern is expected with a resultant difference in distribution of volcanic products. (Abstract of a paper presented at the April 1970 meeting of the American Geophysical Union.)

5. Thermal and Stress History of the Moon

Anderson, A. T., Jr., Newton, R. C., and Smith, J. V.: 'A Possible Petrologic History of the Moon', *EOS* **51**, 348.

From chemical, mineralogic and textural features of Apollo-11 rocks, taken in relation to the Surveyor analyses, the mass and the moment of inertia, we propose a possible petrologic history involving early melting of the Moon. Chemical differentiation involving a metal (plus sulfide?) core, olivine- and pyroxene-mantle, plagioclase-rich highlands and a final Fe, Ti rich liquid plus ilmenite and pyroxene cumulate explains many properties. Although extensive loss of volatiles at the Moon's surface might explain the high content of refractory elements, the low density of the Moon compared to Earth suggests an earlier stage of differentiation before accretion. Crystal-liquid differentiation of a convecting liquid of initial ultra-basic composition produced Mg-rich olivine and then pyroxene which sank towards the center. Ultimately plagioclase floated upwards forming much of the highlands. Impact melted a liquid-pyroxene-ilmenite mixture which then crystallized into the ferrobasalts and microgabbros of the Sea of Tranquillity. (Abstract of a paper presented at the April 1970 meeting of the American Geophysical Union.)

Cook, A. H.: 'The Earth as a Planet,' *Nature* **226**, 18–20.

A comparison of the Earth with the Moon and other planets can help considerably in the solving of

geophysical problems. Professor Cook deals with some of these problems in this article, which is a summary of the inaugural lecture he gave as professor of geophysics at Edinburgh on January 15.

Dietz, E. D. and Vergano, P. J.: 'Origin of Glass Deposits in Lunar Craters', *Science* **168**, 609–610.

Gold's hypothesis on the source of lunar glazing is not consistent with what is known concerning the melting kinetics of plagioclase feldspars, which are primary minerals in basalts. Melting rates are governed by diffusion or viscosity effects. Estimates based on heat flow will be high by orders of magnitude. Droplets which have run down an inclined surface can only have melted in situ if they originated from material different in chemical composition from the unmelted aggregate. On the other hand, the various glazing effects and the presence of glassy spheres are consistent with the hypothesis that both the spheres and the glaze are deposited on impact of relatively fluid molten material. The question of whether the glazing of lunar soil occurred by melting in situ or by the splattering of molten rock should be resolved by the chemical analysis of the glaze, some droplets, and their substrate soil.

Gilvarry, J. J.: 'Thermal History of the Moon,' *Nature* **225**, 623–625.

The approximation to the central temperature set by the result of Ness is used in order to correct previous solutions of the heat-conduction equation, to infer possible thermal histories consistent with the present thermal regime. The present results abundantly indicate that a relatively cold thermal regime in the Moon over roughly the last 3.5 Gyr can be justified consistently with observed levels of radioactivity in terrestrial rocks, without resort to the drastic suggestion of Moon formation antedating that of the Earth by several milliard years (milliard = one thousand million).

Gold, T.: 'Origin of Glass Deposits in Lunar Craters', *Science* **168**, 611.

The solar flash heating was proposed because, in detail, each explanation offered for the phenomenon of surface glazing concentrated in the center of small lunar craters seems unsatisfactory. There are admittedly some events invoked for which there is no other evidence. But we can now determine experimentally by means of the lunar material what the intensity and duration of a flash would need to be to produce the observed effect.

Green, J.: 'Origin of Glass Deposits in Lunar Craters', *Science* **168**, 608–609.

The mechanism of solar flash heating for creating a glaze within small and shallow lunar craterlets in the Apollo-11 landing site, as suggested by Gold, should produce even greater thermal effects in larger and deeper craters, and in craters with much smaller diameter-depth ratios. These melt phenomena should also be dependent on the latitude of the crater. Furthermore, the flare must have been within a small temperature range at about 1325 K on the lunar surface. The author suggests another mechanism for producing glassy objects by the impact of volcanic bombs. During its travel, such a bomb could form a cooled solid skin. Due to the low cooling rate by conduction, this crust then could preserve a molten interior. At the impact, large (> 10 cm) bombs could burst, splatter, and chill to glass. Maximum distance and travel times of volcanic bombs can be much greater, and, for a given range, the bombs could have six times the volume of those of the Earth, given equivalent volcanic energies.

Grossman, J. J., Wegner, M. W., Ryan, J. A., and Mukherjee, N. R.: 'Surface Properties of Apollo-11 Lunar Samples', *EOS* **51**, 345.

Lunar materials previously exposed to dry Nitrogen disrupted when exposed to reactive gases like O₂ and H₂O. Specimens of rock that were fractured in ultrahigh vacuum exhibited a time-dependent adhesion and a network of localized electrostatically charged areas. Electron microprobe composition profiles at grain boundaries indicate rapid cooling of many particles in the soil sample. High defect

densities have been found by preferential chemical etching due to material dislocations, solar cosmic rays, and galactic cosmic rays. Isolated dislocations are found as well as slip plane arrays and slip bands the latter due to plastic deformation at high temperatures. These observations provide a basis for a preliminary analysis of the agglomeration and disruption processes occurring on the Moon and the origin of the adhesive forces. Van der Waals forces, electrostatic charging, and chemically-induced strain release fracturing have been observed. The only agglomeration process not observed yet is low temperature vacuum sintering. (Abstract of a paper presented at the April 1970 meeting of the American Geophysical Union.)

Lowman, P. D., Jr.: 'Crystalline Rocks from Mare Tranquillitatis: Preliminary Petrologic Inferences', NASA-Technical Memorandum-X-63916; X-644-69-550.

Preliminary petrographic studies were made of two crystalline rock samples returned from Mare Tranquillitatis by the Apollo-11 mission, and a discussion of their petrologic implications is presented. Sample 10017 is a finegrained vesicular Type A rock with the following volumetric composition: clinopyroxene, 49.7%; plagioclase, 18.0%; ilmenite and other opaques, 23.9%; interstitial material, 8.3%; and traces of an unidentified mineral. Sample 10047 is a coarser-grained non-vesicular holocrystalline Type B rock with the following composition: clinopyroxene, 4.9%; plagioclase, 32.5%; ilmenite and other opaques, 15.2%; cristobalite, 2.5%. Neither sample showed any evidence of shock. The samples appear representative of the Apollo-11 samples in general and at least locally of the Mare Tranquillitatis bedrock. The crystalline rocks are deduced to be true igneous rock, formed from internally-generated magma, rather than impact melts. The magma is believed to have been primary, and very hot, dry, and fluid by terrestrial standards. The rocks chemically resemble titanium-rich pyroxene gabbros from the Adirondack anorthosite complex. Their petrology implies that the interior of the Moon went through a high temperature stage (1300° to 1500°C) very early in its history.

Papanastassiou, D. A., Wasserburg, G. J., and Burnett, D. S.: 'Rb-Sr Ages of Lunar Rocks from the Sea of Tranquillity', *Earth Planetary Sci. Letters* **8**, 1-19.

⁸⁷Rb-⁸⁷Sr internal isochrons have been determined for six crystalline rocks from the Sea of Tranquillity and all yield ages within the narrow range $3.65 \pm 0.06 \times 10^9$ yr. Differences in initial (⁸⁷Sr/⁸⁶Sr)_I define at least two main rock groups which coincide with the two groups indicated by alkali content of the rocks. This demonstrates that at least two magmatic reservoirs were involved in the 3.65×10^9 yr event on the Moon. The soil yields a model Rb-Sr age of 4.6×10^9 yr which suggests that it consists of an average over a variety of rock systems of different ages which represent a closed total system 4.6×10^9 yr old or the widespread existence of rocks of 4.6×10^9 yr age. A single peculiar rock fragment from the soil gives a model age of 4.4×10^9 yr. Initial Sr compositions for the lunar rocks and for soil fragments define a narrow range (0.6990-0.6994) whose lower limit is equal to the basaltic achondrite initial Sr. The Moon, Earth and basaltic achondrites represent planets with Rb/Sr much lower than in the Sun. The Moon and the basaltic achondrites must have separated from the solar nebula within a time interval of less than 4×10^6 yr. From consideration of Sr-Rb relations, if the Moon formed by fission from the Earth, it must have occurred prior to 4.4×10^9 yr ago.

Papanastassiou, D. A. and Wasserburg, G. J.: 'Rb-Sr Ages from the Ocean of Storms', *Earth Planetary Sci. Letters* **8**, 269-278.

Rb-Sr Internal isochrons for two texturally and mineralogically distinct crystalline rocks returned by Apollo-12 yield similar ages of 3.36 ± 0.10 and 3.26×10^9 years. The initial Sr compositions determined are relatively primitive but distinct so that these samples represent two different rock bodies. These ages are slightly but distinctly younger than the Mare Tranquillitatis Rb-Sr ages and indicate that the flooding of the maria may have occurred only during a short interval of $\sim 300 \times 10^6$ years duration 3.6×10^9 years ago. The soil at the Ocean of Storms yields a well determined model age of 4.44×10^9 years and therefore the special nature and older age of the lunar soil determined at the Apollo-11 site is found to be a widespread phenomenon. Initial Sr compositions from Apollo-12 support our previous conclusion based on Apollo-11 measurements that the Moon as a whole has a Rb/Sr ratio much lower than that in chondrites.

Ringwood, A. E.: 'Petrogenesis of Apollo-11 Basalt and Internal Constitution of the Moon', *EOS* **51**, 348.

Evidence is presented supporting the hypotheses that Apollo-11 basalts formed by a small degree of partial melting deep within the lunar interior rather than by surface impact fusion. This hypothesis has then been tested by an experimental determination of sub-solidus and melting phase relationships in average Apollo-11 basalt over the ranges 0–30 kb and 1000–1500°C. The basalt transforms to eclogite at an unusually low pressure —12 kb at 1100°C. The deeper regions of some maria may be composed of eclogite thus explaining the existence of mascons. The high density of the eclogite (3.74 gm/cm³) precludes Apollo-11 basalt from being a major component of the Moon. Compositions of near-liquidus phases have been determined using an electron-probe microanalyzer. The data, in conjunction with the mean density and moment of inertia of the Moon provide strong constraints upon the mineralogy and composition of the source region from which the basalts were derived. The source region was probably composed largely of orthopyroxene and sub-calcic clinopyroxene (7% CaO, 4% Al₂O₃, Fe/(Fe + Mg) = 0.25) together with some olivine. Source material of this composition would be capable of generating Apollo-11 basalt by about 3% of partial melting at depths of 200–400 km. This source material may be representative of the lunar interior, since it explains the observed mean density and moment of inertia of the Moon. (Abstract of a paper presented at the April 1970 meeting of the American Geophysical Union.)

Wellman, T. R.: 'Gaseous Species in Equilibrium with the Apollo-11 Holocrystalline Rocks During Their Crystallization', *Nature* **225**, 716–717.

Crystallization probably took place at depths greater than a few centimetres and no more than two kilometres. The total pressure, which was equal to the gas pressure in the vesicles and vugs of the Apollo-11 rocks, was therefore between 0.01 and 100 atmospheres. The following conclusions may be drawn from the data: (1) Graphite is stable only at total pressures above about 70 atmospheres and is therefore probably absent from the Apollo-11 samples. (2) Only H₂, H₂O, N₂, CH₄, CO, CO₂, and noble gases are likely to contribute significantly to the vesicle gas pressure. (3) H₂ is more abundant than H₂O and CO is more abundant than CO₂, as would be expected in a highly reducing environment. (4) CH₄ can only be a significant constituent at the higher pressures. (5) N₂ and the noble gases are not significantly restricted by gaseous reactions.

6. Chemical Composition of the Moon

Abell, P. I., Eglinton, G., Maxwell, J. R., Pillinger, C. T., and Hayes, J. M.: 'Indigenous Lunar Methane and Ethane', *Nature* **226**, 251–252.

Samples of Apollo-11 lunar fines have been examined by crushing the sample in vacuum and examining by mass spectrometry the gases released, and by treating the sample with DCl and analysing the isotopic compositions of the methane and ethane. The greater part of the methane and ethane released by crushing or acid treatment of the fines arises from reactions brought about during the experiments. It is likely that hydrolysis of carbides, chiefly cohenite (iron, nickel carbide), is the main source of these hydrocarbons, as shown by the evolution of CD₄, C₂D₆ and almost completely deuterated hydrocarbons. Most of the remainder of the methane and ethane is completely unlabelled, proving that this fraction must have been present as such in the fines.

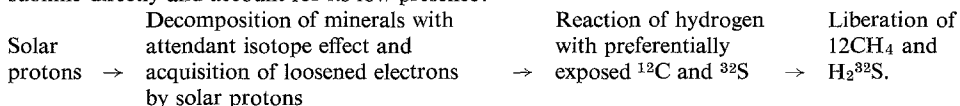
Ahrens, L. H. and Danchin, R. V.: 'Lunar Surface Rocks and Fines: Chemical composition', *Science* **167**, 87–88.

A critical examination of the chemical abundance data on 12 specimens of lunar surface material has led to the following conclusions: (1) Because of the uniformity of chemical composition in the specimens, average values are significant despite small numbers of analyses. (2) The chemical composition

of the Tranquillity Base samples is unlike any known terrestrial rock or meteorite, but shows some distinct euclritic abundance features. The elements discussed are: Si, Fe, Ca, Al, Ti, Mg, Na, Cr, Mn, and K.

Berger, R.: 'Reaction of Carbon and Sulphur Isotopes in Apollo-11 Samples with Solar Hydrogen Atoms', *Nature* **226**, 738-739.

The following reaction scheme is proposed with the understanding that some of the sulphur may sublime directly and account for its low presence:



Bogard, D. D., Funkhouser, J. X., Schaeffer, O. A., and Zahringer, J.: 'Xenon and Krypton Abundances in Lunar Material Returned by Apollo-11 and Apollo-12', *EOS* **51**, 345.

The abundances and isotopic composition of xenon and krypton have been determined in more than forty samples of fine material, breccia, and crystalline rocks returned by Apollo-11 and Apollo-12. The dominant noble gas component in the fines and breccia is of a solar wind origin, whereas the dominant component in the crystalline rocks arises from cosmic ray interactions. Solar krypton is similar isotopically to krypton trapped in carbonaceous chondrites, whereas solar xenon is depleted in its two heaviest isotopes. The spallation spectra of krypton and xenon is similar to that found in calcium-rich achondrites. However, certain isotopes, and especially ^{131}Xe , show significant differences which are probably the result of a lower energy cosmic ray spectrum in these rocks. Amounts of spallation-produced ^{126}Xe are consistent with the radiation ages. (Abstract of a paper presented at the April 1970 meeting of the American Geophysical Union.)

Carter, J. L. and MacGregor, I. D.: 'Chemistry and Morphology of Lunar Sample Surface Features', *EOS* **51**, 345.

The presence of breccias, glasses, glass spattered surfaces, numerous glass lined craters on rock surfaces and shocked rock and mineral fragments suggests a complex history of impacts, and shows that both the impacting and impacted objects varied from liquids to solids implying the presence of an impact produced cloud of gas, liquid, and solid particles. Scanning electron microscopy of glass spheres reveals impact craters down to one micron, splash glasses, dimples, and mounds down to less than 0.05 microns that may be arranged in geometrical patterns. Probe analyses of the mounds showed them to be comprised of metallic Fe, FeS, or aggregates of metallic Fe-Ni spherules in FeS. The mound are probably surface expressions of droplets that formed from the contraction of immiscible surface films which condensed onto drops of volatile-rich liquid silicates. Solidification and subsequent expulsion of a droplet left a dimple with a characteristically textured surface, and an inner dimple with a smooth surface that probably formed from trapped volatiles. The chemistry of the glass spheres and splashed glasses is highly variable, whereas the glass in the center of the small impact craters is essentially isochemical with its host. The high iron and nickel content of some mounds suggest that the projectiles were in part iron or nickel iron. (Abstract of a paper presented at the April 1970 meeting of the American Geophysical Union.)

Clark, J. R., Ross, M., Appleman, D. E., Papike, J. J., and Bence, A. E.: 'Fe/Mg Distribution in a Lunar Pigeonite', *EOS* **51**, 436.

About 770 X-ray diffraction data have been used in least-squares refinement of structural parameters and Fe/Mg distribution in the M1 and M2 sites of a lunar pigeonite crystal from rock 10003, starting with parameters of a refinement for pigeonite (Isle of Mull, Scotland) by Morimoto and Güven. From intensities on X-ray diffraction photographs, the lunar crystal is estimated to be about 90 atom % pigeonite, 10 atom % augite. (Abstract of a paper presented at the April 1970 meeting of the American Geophysical Union.)

Cohen, A. J.: 'Radiation-induced Changes in Iron in Lunar Crystalline Rock', *EOS* **51**, 345.

Changes in the absorption spectra of Fe^{2+} and Fe^{3+} , induced in polished thin-sections of Apollo-11 rocks, in air, by light, by X-irradiation, and by heat are interpreted. In general, light (Xe-Hg lamp) causes oxidation of Fe^{2+} to Fe^{3+} (increased reddening). Subsequent X-irradiation produces metastable iron-related color centers at intrinsic Fe^{3+} sites. On standing, the metastable centers decay to regenerate Fe^{3+} ion. Additional centers decay on heating at 200°C , accompanied by reduction of Fe^{3+} and probable oxidation of Ti^{3+} to Ti^{4+} . Heating at 500°C causes large-scale oxidation of Fe^{2+} to Fe^{3+} . The minerals responsible for the changes will be discussed and mechanisms involved will be compared to those in Fe^{2+} - and Fe^{3+} -doped synthetic quartzes under similar conditions. (Abstract of a paper presented at the April 1970 meeting of the American Geophysical Union.)

Davis, P. K., Kaiser, W. A., Lewis, R. S., and Reynolds, J. H.: 'Rare Gases from Stepwise Heating of Neutron Irradiated Apollo-11 Samples', *EOS* **51**, 345.

In our first work on Apollo-11 samples we examined all the rare gases released in stepwise heating of a sample of lunar fines ($\neq 84$) and of two lunar rocks ($\neq 57$ and $\neq 44$). The data permitted us to identify and to measure compositions and amounts of trapped gases, cosmogenic gases, radiogenic argon-40, and fissionogenic xenon. Apparent small excesses of xenon-128, xenon-129, and krypton-80 were also detected not in correlation with the cosmogenic gases. We are continuing this work by examination of the gases from stepwise heating of neutron irradiated specimens of these samples. We shall report K-Ar ages by the argon-40/argon-39 method and shall report concentration (in gas retentive sites) of bromine and iodine. (Abstract of a paper presented at the April 1970 meeting of the American Geophysical Union.)

Eugster, O., Tera, F., Burnett, D. S., and Wasserburg, G. J.: 'The Isotopic Composition of Gd and the Neutron Capture Effects in Samples from Apollo-11', *Earth Planetary Sci. Letters* **8**, 20-30.

The isotopic composition of Gd in six rocks, one breccia, two core samples, and soil has been determined. Isotopic variations due to capture of low energy neutrons produced by cosmic ray interactions have been found in all samples except for two rocks. Using cosmic ray exposure ages, the effective thermal neutron fluxes were calculated using a nominal value of $157\sigma = 2.62 \times 10^5$ barns. They vary from less than $0.27n/\text{cm}^2 \text{ sec}$ to $1.1 n/\text{cm}^2 \text{ sec}$ indicating variable shielding for the samples studied. The neutron dosage of the top and the bottom of core $\neq 2$ is the same. This means that the soil has been mixed to 13 cm at least once in the last 100 million years. A mixing depth of 23 to 47 m can be calculated based on the integrated effective thermal neutron dosage of $9 \times 10^{15} n/\text{cm}^2$ for the soil and an assumed surface flux of $0.2 n/\text{cm}^2 \text{ sec}$. For rock $\neq 17$ the barium isotopic composition was determined and found to be the same as terrestrial to within 0.1% for the five abundant isotopes.

Funkhouser, J. G., Schaeffer, O. A., Bogard, D. D., and Zahringer, J.: 'Rare Gas Analyses of Apollo 11 and 12 Core Tube Samples', *EOS* **51**, 345.

The results of replicate rare gas analyses of samples selected at different levels in four core tubes from Apollo 11 and 12 are presented. Both rare gas abundances and isotopic ratios are generally similar to composite results for the surface fine material at the two different landing sites. The noble gas content in several isolated rock fragments and in the coarse crystalline stratum of the Apollo-12 long core tube resembles that found in many of the surface rocks. Thus exposure ages can be deduced and used to set limits on rates of deposition. (Abstract of a paper presented at the April 1970 meeting of the American Geophysical Union.)

The Lunar Sample Preliminary Examination Team,: 'Preliminary Examination of Lunar Samples from Apollo-12', *Science* **167** 1325-1339.

The major findings of the preliminary investigation are reported. The conclusions concerning rocks from Tranquillity Base also apply to the Apollo-12 rocks except the Apollo 12 site appears to be less

geomorphologically mature, with a thinner regolith and lower amount of solar wind material in the fines; the $^{40}\text{K}/^{40}\text{Ar}$ age of the mare material in Oceanus Procellarum is about 1 billion years younger; the Apollo-12 rocks contain less Ti, Zr, K, Rb and more Fe, Mg, Ni; and, most of the igneous rocks fit a fractional crystallization sequence. There are also differences in texture, stratification, indigenous organic material and distribution of elements between crystalline rocks and fines.

Mueller, R. F.: 'Apollo-11 Evidence for the Differentiation of Lunar Materials', *Nature* **226**, 925–927.

The compositions of the surface rock at Tranquillity Base seem to be consistent with a differentiation mechanism, perhaps of a complex character embodying igneous and other processes, but which probably contained elements similar to that which produced the crust of the Earth. There are important modifications induced by the low water content of the lunar rocks, however.

Mueller, R. F.: 'Chemical Differentiation of Venus, Earth, and the Moon', *EOS* **51**, 344.

Comparative studies of Venus, Earth and the Moon point to major contrasts in the types of differentiation of these planets, depending on their temperatures and water contents. High temperatures on Venus do not lead to widespread occurrence of melts, but they do imply basification of the subcrust through partial fusion as well as slower cooling rates, which favor igneous and metamorphic differentiation at shallower depths than on Earth. These high temperatures and analogies with Earth also imply that differentiation processes are operative on Venus at present. However, the hydrogen escape rate on this planet indicates that these processes may have been more effective in the past than at present since they are favored by water. On the Moon, where most differentiation probably occurred in the remote past, low water content may have inhibited the marked concentration of feldspathic components characteristic of terrestrial continental rocks. Mechanism for the upward concentration of FeO by magmatic processes, with consequent density inversions exist on all three planets. On the Moon these processes can account for the high surface densities. However, on Venus high temperatures tend to inhibit such gravitational instabilities by weakening the crust. On the Moon, compositional differences, low mean surface temperatures, and short time scale of magmatic processes probably favored gravitational instabilities. (Abstract of a paper presented at the April 1970 meeting of the American Geophysical Union.)

Nagy, B., Scott, W. M., Modzeleski, V., Nagy, L. A., Drew, C. M., McEwan, W. S., Thomas, J. E., Hamilton, P. B., and Urey, H. C.: 'Carbon Compounds in Apollo-11 Lunar Samples', *Nature* **225** 1028–1032.

The Apollo-11 lunar samples contain traces of carbon compounds. Pyrolysis experiments of both lunar fines and the interior of a lunar breccia showed CH_4 , $\text{C}_2\text{-C}_5$ hydrocarbons, CO_2 , as well as aromatic compounds: benzene, toluene, *o*, *m* and *p*-xylenes, ethylbenzene, styrene, indene, naphthalene, biphenyl, thiophene and several methyl substituted isomers. At least some of the aromatic hydrocarbon products could have been synthesized by pyrolysis. It has been reported that basically the same aromatic hydrocarbons are obtained when methane is heated at higher temperatures (1000°C) over silica gel. The following possible origins of carbon compounds on the Moon are considered. (1) The accumulation of carbon and hydrogen from the solar wind. (2) The accumulation of carbon from carbonaceous meteorite and cometary impacts. (3) The possibility of a primitive atmosphere. (4) The possibility that the carbon compounds originate from the degassing of the Moon.

Nayak, V. K.: 'Geoplanetology: A New Term for Geology of the Planets Including the Moon', *Geol. Soc. Am. Bull.* **81**, 1279–1280.

Faced as we are with increasing amounts of significant geological information of the Moon's surface, its rocks and soil samples, it seems desirable to furnish new terminology to convey exact measuring and to avoid confusion which may arise by using varied terms for geological study of not only the Moon but also other planets. The author proposes the term 'Geoplanetology' to cover geological and related aspects of the Moon and other planets which are likely to be investigated in the future.

O'Keefe, J. A.: 'Tektite Glass in Apollo-12 Sample', *Science* **168**, 1209-1210.

The glassy portion of lunar sample 12013 from Apollo-12 is chemically more like some tektites from Java than like any terrestrial igneous rock. It satisfies all the chemical criteria for a tektite. Tektites are relatively recent and acid rocks, whereas the Moon is chiefly ancient and basaltic; hence, tektites are probably ejected volcanically, rather than by impact, from the Moon.

O'Keefe, J. A.: 'Geochemical Evidence for the Origin of the Moon', *EOS* **51**, 350.

The Apollo 11 and 12 studies show that the lunar surface is depleted in siderophile elements. Since the dynamic behavior of the Moon indicates that it has no core, the simplest explanation is that the Moon was formed by the fission of the Earth after the siderophiles had gone to form the core. The Moon's surface is even more deficient in water and other volatile elements than the Earth; it is enriched in refractory elements. This is attributed to the loss of most of the initial mass of the Moon as a result of heating by tidal friction after fission. The hypothesis is supported by the evidence of early internal heating. The evidence that the Moon was formed by fission suggests that perhaps fission has been a fundamental process in the formation of the solar system; in general, planetary processes result in breakup rather than accretion. (Abstract of a paper presented at the April 1970 meeting of the American Geophysical Union.)

Patterson, J. H., Turkevich, A. L., Franzgrote, E. J., Economou, T. E., and Sowinski, K. P.: 'Chemical Composition of the Lunar Surface in a Terra Region near the Crater Tycho', *Science* **168**, 825-828.

More precise and comprehensive analytical results for lunar surface material in a terra region have been derived from the data of the α -scattering experiment on Surveyor-7. The silicon content and the low sodium abundance are close to that of mare material. The abundances of titanium and iron are at least a factor of 2 lower, whereas the abundances of aluminum and calcium are significantly higher. The analytical results provide direct evidence for chemical differentiation in the Moon and indicate a lunar crust of appreciably lower density than the whole Moon and with lower density and higher albedo than lunar mare material.

Ringwood, A. E.: 'Origin of the Moon', *EOS* **51**, 346-347.

Chemical compositions of Apollo-11 basalts and terrestrial basalts and of their respective source regions are compared. Principal similarities are (1) both source regions are composed dominantly of Mg-Fe silicates with lesser Ca and Al (2) both source regions are characterized by strong depletions of relatively volatile metals, e.g. Na, K, Rb, Cs, Pb, Zn, Cd, In, Bi, Sb, Ge, when compared to the primordial abundances. Superimposed on these overall similarities are some major differences in mineralogy, chemical composition, Fe/(Fe + Mg) ratio and oxidation state. The Apollo-11 basalt source region has been depleted in the above volatile elements compared to the terrestrial basalt source region by factors of 3 to 100. Apollo-11 basalts on the average also display marked depletion of siderophile elements compared to terrestrial basalt. These compositional differences are difficult to explain on the basis of the traditional direct fission, binary planet and capture theories of lunar origin, and alternative theories are required. It is suggested that in the later stages of accretion of the Earth, a massive primitive atmosphere was developed and the temperature was sufficient to evaporate selectively a substantial proportion of the silicates falling on the Earth. The primitive atmosphere was subsequently dissipated as the Sun passed through a T-Tauri phase. Rotational instability due to core formation in the Earth may also have been. (Abstract of a paper presented at the April 1970 meeting of the American Geophysical Union.)

Salisbury, J. W. and Logan, L. M.: 'The Composition of the Moon: Evidence for Heterogeneity', *Meteoritics* **4**, 206.

The recent chemical analyses of lunar surface material performed by the Surveyor spacecraft have indicated a very similar composition for three different areas on the lunar surface. Consequently, it is a widespread belief that the Moon, or at least its surface, is homogeneous. The Surveyor α -scattering

analysis is shown, however, to be insufficiently precise to allow such a conclusion to be drawn. Spectroscopic data in the visible, near-infrared and mid-infrared regions of the spectrum show very clearly that the surface is not homogeneous. This heterogeneous composition of the lunar surface layer implies differentiation of the Moon and a complex, rather than simple, geological history. (Abstract Only.)

Silver, L. T.: 'Lead Isotopic Heterogeneity in Lunar Soil 10084,35 and its 'age' implications', *EOS* **51**, 348.

Fractional extractions of lead, uranium and thorium from Tranquillity Base soil sample 10084,35 have been made by acid leaching, vacuum volatilization and mineral separations. Acid leaches in two experiments have demonstrated that the isotopic composition of lead in the soil (a) is in a variety of sites; (b) is incredibly heterogeneous with Pb^{207}/Pb^{206} ratios in the radiogenic components of differentiates varying by at least a factor of 1.5; and (c) is a composite derived from various materials in uncertain proportions and is not uniquely susceptible to age interpretation. The uranium and thorium are also distributed in various sites with variable Th/U ratios and show different labilities than the leads during acid leaching. Vacuum volatilization provides a different pattern of lead isotope mobilization than the acid leaches, confirming a variety of lead sites in the soil. The 4.6–4.7 billion year 'ages' found for the soil from U-Th-Pb systematics are *apparent*, only. Present data permits several diverse possible interpretations; an exciting one is that the Moon may be older than 4.9 billion years, but should be treated with caution. Similar cautions might be applied to other radiogenic isotope systems in the soils from which 'ages' for the Moon have been inferred. (Abstract of a paper presented at the April 1970 meeting of the American Geophysical Union.)

Troitskii, V. S., Bondar', L. N., Zelinskaya, M. R., and Strezhneva, K. M.: 'Comparison of the Chemical Composition of Lunar Surface Material Determined by Radioastronomical Observations with the Results of Chemical Analysis Obtained by Surveyor', *Radio Sci.* **5**, 247–251.

The authors compare the results of the chemical analysis of the lunar surface material made by Surveyor with that based on the data of the radio astronomical investigations of the electromagnetic properties of the lunar material.

Turkevich, A. L., Patterson, J. H., Franzgrote, E. J., Sowinski, K. P., and Economou, T. E.: 'Alpha Radioactivity of the Lunar Surface at the Landing Sites of Surveyors 5, 6, and 7', *Science* **167**, 1722–1724.

Evidence has been obtained for a radioactive deposit on the lunar surface at Mare Tranquillitatis with a total intensity of 0.09 ± 0.03 α -disintegration per second per square centimeter. The presence of polonium-210 in amounts that are close to equilibrium indicates a continuous turnover rate of lunar material at this site of less than 0.1 micrometer per year. The lack of such a deposit at two other lunar sites suggests lower local concentrations of uranium there.

Ulbrich, M. C.: 'Chemical Individuality of Lunar, Meteoritic, and Terrestrial Silicate Rocks', *Science* **168**, 1375–1376.

Turner and Ulbrich recently suggested a basis for the chemical comparison of non-terrestrial with terrestrial rocks using atomic ratios such as Ca/Na, (Ca + K)/Na, Fe/Mg, and Al/Ti, which reflect the genesis of rocks. In this note, the author presents some composition fields plotted respectively for appropriate igneous rocks, eucrite meteorites, and lunar surface materials. The Ca/Na vs Fe/Mg plot and the Ca/Na vs Ti plot reveal consistent chemical differences between these three rock types. Perhaps it is time to set up a suitable nomenclature for lunar rocks.

Vinogradov, A. P.: 'On the Composition of Lunar Rocks', *Geochemistry International* **6**, 977–978.

The author makes some comments in this paper about what rock types shall be found on the lunar

surface. The meteoritic composition of terrestrial planets and of the Earth in particular is assumed. A table is presented which shows that the Ca-rich feldspathic achondrites resemble basalts of the Earth's crust in composition as well as in ophitic structure. The conclusion is drawn that the rocks of the surface of the Moon (for instance of seas) are products of fusion of meteoritic matter during the process of volcanic activity and that they must be close to the average composition of feldspathic achondrites approaching terrestrial tholeiitic basalts depending on the differentiation depth.

Windley, B. F.: 'Anorthosites in the Early Crust of the Earth and on the Moon', *Nature* **226**, 333–334.

Although there are many unknowns concerning these early Pre-Cambrian calcic anorthosites, it is important to recognize their existence as an integral group. On account of their extreme age, their compositional similarities with the lunar anorthosites and dissimilarities with other known terrestrial igneous rocks (chemically they are only comparable with the chromiferous grossphidite inclusions in kimberlite pipes), it is suggested that they are fragments of (primordial?) layered differentiates formed early in the evolution of the Earth. This suggests that both planetary bodies went through parallel stages of development as far as the anorthosite event is concerned, and thus that the Moon may not be so dissimilar to the Earth as previously suspected.

7. Lunar Exosphere

Balsiger, H., Freeman, J. W., Jr., and Hills, H. K.: 'Preliminary Results from the Apollo-12 ALSEP Lunar Ionosphere Detector: II. The Ion Mass Spectrometer', *EOS* **51**, 407.

The Apollo-12 ALSEP ion mass spectrometer measures the crude mass per unit charge spectrum from 10 to 1000 AMU/q for ions in the energy range from 0.2 to 48.6 eV. Mass spectra of ions of energy 48.6 eV are available from early in the experiment life. These spectra show a concentration of ions in the 18 to 50 AMU/q mass per unit charge range. Several possible sources for these medium mass ions such as LM exhaust products and sputtered or thermalized solar wind ions will be discussed. (Abstract of a paper presented at the April 1970 meeting of the American Geophysical Union.)

Freeman, J. W., Jr., Balsiger, H., and Hills, H. K.: 'Preliminary Results from the Apollo-12 ALSEP Lunar Ionosphere Detector – I. General Results', *EOS* **51**, 407.

Salient features from the lunar ionosphere detector at the lunar surface include the following: (1) There is a frequent appearance of ions in the ten to several hundred eV energy range. These ions come and go in a cloud-like fashion. Often the onset of such clouds of ions is accompanied by the presence of higher energy ions. There is a strong suggestion of solar wind acceleration of ambient ions of either natural or LM associated origin. (2) Energetic ions are seen in good time correlation with the impact of the LM ascent stage into the lunar surface. Again there is a strong suggestion that the impact-released gases have been ionized and accelerated by the solar wind. (3) High background counting rates seen during the lunar day may be indicative of large quantities of gas escaping from the LM descent stage tanks. (Abstract of a paper presented at the April 1970 meeting of the American Geophysical Union.)

Manka, R. H. and Michel, F. C.: 'Lunar Atmosphere as a Source of Argon-40 and Other Lunar Surface Elements', *Science* **169**, 278–280.

The lunar atmosphere is the likely source of excess argon-40 in lunar surface material; about 8.5% of the argon-40 released into the lunar atmosphere will be implanted in the surface material by photoionization and subsequent interaction with fields in the solar wind. The atmosphere is also likely to be the source of other unexpected surface elements or of solar wind elements that impact from non-solar wind directions.

Manka, R. H. and Michel, F. C.: 'Lunar Atmosphere as a Source of Ar⁴⁰ and Other Lunar Surface Elements', *EOS* **51**, 344.

Based on calculations of lunar ion trajectories, we suggest that the lunar atmosphere is very likely the source of Ar⁴⁰ in lunar surface grains. Ar⁴⁰ is thought to come from decay of K⁴⁰ in the Moon and subsequent diffusion into the atmosphere where it can be ionized. The ion interacts with the solar wind and in the lunar frame of reference the mechanism for impact is primarily acceleration by the interplanetary and lunar surface electric fields. Impact energies up to several kilovolts are found which are sufficient for effective implantation in lunar soil grains. However, the flux is found to be in a direction perpendicular to the solar wind flow. Other applications to lunar samples are mentioned. (Abstract of a paper presented at the April 1970 meeting of the American Geophysical Union.)

Manka, R. H. and Michel, F. C.: 'Energy and Flux of Ions at the Lunar Surfaces', *EOS* **51**, 408.

We examine the acceleration of ions in the lunar atmosphere by the interplanetary electric field. For the sunlit lunar surface, ions formed in one hemisphere travel nearly vertically along the interplanetary electric field and impact the Moon with energies up to a few kilovolts; ions formed in the other hemisphere are lost. The direction of the flux reverses when the polarity of the interplanetary magnetic and electric fields change. Thus we predict an energetic, highly directional, lunar ion flux but with the possibility that light ions such as hydrogen can execute orbits that return them to portions of the lunar surface not directly exposed to the solar wind. Applications to Apollo experiments will be given. (Abstract of a paper presented at the April 1970 meeting of the American Geophysical Union.)

Mihalov, J. D., Colburn, D. S., and Sonett, C. P.: 'Observations of Magnetopause Geometry and Waves at the Lunar Distance', *Planetary Space Sci.* **18**, 239-258.

Magnetic observations at the lunar distance of the magnetopause, or boundary between the geomagnetic tail and the magnetosheath, are surveyed. The boundary surfaces are shown to have normal vectors from which an average tail aberration induced by the Earth's heliocentric motion of $9 \pm 5^\circ$ and a flaring half-angle of $\sim 9^\circ$ is found. The boundary is assumed to be a tangential discontinuity. The average ecliptic diameter of the tail at lunar distance is 50 Earth radii. Using 21 normal vectors, a statistical variation transverse to the tail axis three times that along the axis is shown. This may correspond to magnetic perturbations induced by the Kelvin-Helmholtz instability; the variations of the unit normals are consistent with circumferential oscillations having wavelengths smaller by $1/3$ to $1/10$ than those of waves moving in the downstream direction. The circumferential oscillations appear to give evidence of fluting of the tail surface. Several distinct types of boundary signature are identified. Boundary speeds which usually exceed typical spacecraft velocities of ~ 1 km sec⁻¹ are deduced from simple models of boundary motion. Implied boundary thicknesses are usually ~ 1000 km, but perhaps are as low as ~ 30 km in some instances. Use of K_p as an indicator of solar wind conditions does not reveal correlation with the number of multiple crossings or the changes in magnetic field magnitude across the boundary.

Rozenberg, G. V.: 'Atmospheric Pressure on the Moon from the Data of Twilight Photography with Surveyor-7', *Astron. Zh.* **47**, 449-453.

On the basis of the analysis of the image of the twilight horizon, transmitted by Surveyor-7 from the lunar surface, the upper estimation of the air density at the height of about 10 m above the lunar surface, is obtained.

Singer, S. R.: 'Use of Lunar Data to Determine Space Erosion of Meteorites', *Meteoritics* **4**, 294.

Meteorites in space are eroded mainly by micrometeorite impacts. Erosion rates of 5×10^{-8} to 5×10^{-7} cm/yr have been proposed for iron and stone meteorites, resp. (Whipple, Fireman, Fisher). The process can be scaled for rocks on the lunar surface to take account of differences in flux, impact velocity, and secondary effects. An experimental check is provided by measuring the concentration of Al²⁶ as a function of depth (from the present surface of the rock), on a millimeter scale. (Abstract only).

Whang, Y. C.: 'Observations of the Lunar Mach Cone', NASA-Technical Memorandum-X-63843; X-692-70-60.

The region of penumbral decreases of the magnetic field in the lunar wake is bounded on its exterior by a Mach cone tangential to the lunar body. The existence of such a lunar Mach cone has been confirmed by magnetometer data from lunar Explorer-35. The axis of the Mach cone indicates that the direction of the solar wind comes from approximately 4.5° west of the Sun as viewed from the Moon. With the direct measurements of the solar wind speed, this indicates that the azimuthal velocity is approximately 5 km/sec in the sense of the solar rotation. Due to the variability of the magnetic field direction, the spacecraft has actually observed the three-dimensional wake region of the interaction of the solar wind with the Moon. The lack of axial symmetry of the observed lunar Mach cone provides the first experimental evidence for the anisotropic propagation of magnetoacoustic waves in the solar wind. The average Mach angle is found to be approximately 8° in directions perpendicular to the magnetic field vector, and approximately 5.5° in the direction parallel to the field leading to a velocity anisotropy of approximately 1.4. This compares favorably with the nominal expected value in the solar wind.

Yamashita, Y.: 'Time Dependent Variations in Sky Emission Temperatures at Millimeter Wavelengths', NASA-Contractor's Report-110225; Quarterly Progress Report-3.

8. Lunar Coordinates and Mapping of the Moon

Kisljuk, V. S.: 'A Systematic and Accidental Differences of Selenodetic Networks of Bench Marks', *Astron. Zh.* **47**, 610-611.

The differences of the system of modern catalogues of Basic Points on the lunar surface are given. The dispersion of the positions of these points are estimated for different pairs of catalogues. The correlation between values of absolute heights of common points has been studied.

Kuiper, G. P., Arthur, D. W. G., Connors, H. J., and Baters, P.: 'Research Directed Toward a Photo-telescopic Selenodetic Measuring Program' (Final Report), AFCRL-69-0537.

Lincoln Lab., Mass. Inst. of Tech.: 'Radar Studies of the Moon', NASA Contractor's Report-108302; Quarterly Progress Report-2.

The instrumentation of the two-channel radar receiver is presented. Mounting the Planetary Radar (PR) Box, including an operational two-channel receiver, on the 120-foot antenna is scheduled for four weeks planetary observations. Much of that period will be occupied with tests of the dual-channel system. An intensive mapping operation will begin when the PR Box again is mounted on the antenna. The first-phase (real-time) and second-phase (Fourier transform) computer programs have been rewritten to process the multiplexed two-polarization data and produce one pre-mapping tape for each polarization. As a result, the third-phase (mapping) program can be used without change.

Lincoln Lab., Mass. Inst. of Tech.: 'Radar Studies of the Moon', NASA-Contractor's Report-108303; Quarterly Progress Report-3.

The first few subarea maps have been produced from observations made in November 1968. This Planetary Radar Box was operated for four weeks from October 28 to November 29, following the successful completion of the work on updating the receiver for two polarizations. For the present program, the subarea being mapped as ZAC areas, a more reasonable pseudo-range-doppler subdivision of the Moon's surface, rather than the previous latitude-longitude subdivision into LAC areas. About 12% of the near hemisphere (30 out of 224 ZAC areas) was successfully measured

with a resolution of at least 2.5 km. There were problems, however, with the post-processing computer programs that limited the number of finished maps to about six. The remaining measurements are being processed.

Lincoln Lab. Mass. Inst. of Tech.: 'Radar Studies of the Moon', NASA-Contractor's Report-108 351; Quarterly Progress Report-4.

Measurements continued for the high-resolution lunar maps, and production of the subarea maps was initiated. An investigation of ephemeris anomalies and interpretation of the data was undertaken.

Lipskii, Yu. N. and Nikonov, V. A.: 'The Construction of a Hypsometric Map of the Visible Side of the Moon, Taking into Account a Relief', *Astron. Zh.* **47**, 407-410.

A hypsometric map of the visible side of the Moon, based on Hopmann's catalogue and the U.S. Army Map Service data, has been prepared. The graphic representation of the isohypses has been worked out with consideration of a 1.0 km relief.

Lipskii, Yu. N. and Shevchenko, V. V.: 'The Principles of the Physical Mapping of the Lunar Surface', *Astron. Zh.* **47**, 586-598.

Owing to the intensive investigation of the Moon by various astrophysical methods and direct investigations of it with the help of cosmic apparatus, search of a complex, universal method of generalization of this information and reduction of it to the universal system of data, is urgently needed.

Since at present the principal purpose of investigations in the most cases is the surface of the lunar globe, the physical mapping of the lunar surface can be the most effective form of the analysis of diversified information.

The process of the creation of cartographic pictures of the whole lunar surface or separate regions, containing information on the presence and distribution of various physical characteristics of the lunar surface is described as physical mapping.

Lipskii, Yu, N.: 'Photomap of the Visible Hemisphere of the Moon, 1:5000000 Scale', Gos. Astron. Inst. Im. P. K. Shternberga and Topogeodezicheskaya Sluzhba SSR (Moscow). English Translation in ACIC-TC-1496.

Photomap of the Moon's visible hemisphere was compiled on the basis of original photographs received from native and foreign observatories, with additional materials from photographic atlases of the Moon. The chart was drawn in an oblique, positive, exterior, perspective projection with positive libration values in altitude and longitude close to the maximum, which creates conditions of visibility of the eastern limb zone. This zone connects the visible hemisphere with the western sector of the far side of the Moon, which was photographed by A.M.S. Luna 3 in 1959.

Makarenko, N. L.: 'On the Reduction of the Centre of the Moon Figure to its Centre of Mass', *Astron. Vestnik* **4**, 208-210.

A theoretical possibility of the determination of the position of the centre of the lunar figure in the selenocentric system of coordinates is considered by the use of photographs of the Moon on the background of stars.

Moskowitz, S.: 'Guidance and Control Payload Support Requirements for a Planetary Cartographic Probe', NASA-Technical Note-D-5853.

The guidance and control requirements for payload support of a planetary orbiting cartographic spacecraft were examined. Mapping scales of 1:1000000 and 1:5000000 were selected for the para-

metric study of Lunar, Martian and Jovian cartography. Relations were established between camera pointing angle, field-of-view, and imaging resolution in terms of planetary physical characteristics and mapping scale. From these, orbit selection rules were formulated for orbits of various inclinations with particular attention directed towards those of 30 and 90 degrees (polar orbits). Spacecraft attitude control requirements were then obtained as a function of these parameters and the selected image overlap. The resulting overall guidance and control specifications are described in terms of potential instrumentation subsystem.

Mueller, I.: 'A General Review and Discussion on Geodetic Control of the Moon, Phase 1 Final Report', NASA-Contractor's Report-108301.

Nance, R.: 'Positions of Lunar Features from Apollo-8', *J. Geophys. Res.* **75**, 2029–2039.

From Apollo-8 data, positions were obtained for three lunar far-side features. The positions may be used to improve the accuracy of lunar far-side maps. Based on these positions, the best lunar far-side maps are estimated to be accurate to within 60 km (1σ) in latitude and longitude. The position of an earth-side feature was determined and used to evaluate the accuracy of the Apollo navigation system.

Schaber, G. G., Eggleton, R. E., and Thompson, T. W.: 'Lunar Radar Mapping: Correlation Between Radar Reflectivity and Stratigraphy in North-Western Mare Imbrium', *Nature* **226**, 1236–1239.

Preliminary evaluation of the radar data for the Sinus Iridum quadrangle (32° – 48° N; 14° – 38° W) has revealed that the lowest values of radar reflectivity are closely correlated with the mare materials of lowest albedo mapped by Schaber as of most recent volcanic origin.

Strelitz, R.: 'Lunar Landmark Study', NASA-Contractor's Report-109459.

The results of a preliminary examination of the lunar surface to ascertain its suitability for landmark navigation is presented. The basic technique of landmark navigation is to triangulate the position of the observer by means of bearings to landmarks. A navigation fix is provided relative to the terrain, obviating an intermediate reference to a co-ordinate system. The minimum equipment for landmark navigation required aboard a remotely controlled roving vehicle is an imaging camera and a readout of its pointing angles.

Valeev, S. G.: 'Selenodetic Studies from Positional Observations of the Moon', *Soviet Phys. – Astron.* **13**, 993–996.

Possible solution of several selenodetic problems on the basis of large-scale photographs of the Moon against a background of stars is discussed. Equations are given for transforming from equatorial lunar coordinates to orbital coordinates and back through the use of 'Cracovian' matrices.

9. Morphology of the Lunar Surface

Elston, W. E., Laughlin, A. W., and Brower, J. A.: 'Lunar Near-side Tectonic Patterns from Orbiter Photographs', *EOS* **51**, 346.

Previous studies indicating intense non-random azimuths between centers of intersecting lunar craters > 10 km in diameter (away from the Moon's leading edge, becoming random near the limb) were supplemented by 14000 lineation plots on Orbiter photographs of near-side mare ridges, valleys (including rille segments), and highland ridges (including walls of polygonal craters and walls com-

mon to adjoining craters). N-S lineations are dominant, followed by NE, NW, NNE, and NNW trends. Orbiter resolution modified earlier earth-based observations on the lunar tectonic grid. For example, E-W lineations, prominent among intersecting craters, are conspicuously absent. Supposedly concentric wrinkle ridges in Mare Humorum and lineaments supposedly radial to Mare Oriental and Mare Imbrium lack E-W components. A mechanical model suggesting E-W tension is indicated. (Abstract of a paper presented at the April 1970 meeting of the American Geophysical Union.)

Larsen, P. A. : 'Some Photographic Results of the Apollo-11 Mission', NASA-Technical Memorandum-X-64 501.

The work reported was done for several reasons: (1) to show what types of photographs are available as a result of the Apollo-11 mission; (2) to give the best possible photographic description of the lunar terrain in the vicinity of Tranquillity Base, and as many other areas of the lunar surface as possible, so that Lunar Roving Vehicle mission planners, designers, and engineers can obtain a feel for several types of lunar terrain that may be encountered by the lunar roving vehicle; (3) to show some of the better pictures as single photographs, stereograms, constructed panoramic views, sequence strips, and mosaics; (4) to demonstrate the feasibility of making certain elevation measurements of lunar topographical features, by using lunar photographs, photogrammetric techniques, and locally available photogrammetric equipment; and (5) to provide a reminder of the value of high altitude Earth photography for Earth resources studies. The 1405 photographs taken during the Apollo-11 mission were reviewed. Of this number, 104 were judged to be of sufficient interest for this study, and to warrant further analysis. Consequently, 27 stereograms, 9 panoramic views, one sequence strip, one mosaic, and 17 single photographs are included in this report, together with pertinent interpretations of the photographic data.

Mironova, M. N.: 'Structural Characteristic of Some Craters on the Far Side of the Moon', in: *Astronomy and Astrophysics*, No. 1: *Physics of the Moon and Planets* (ed. by I. K. Koval – Transl. into English of the Publ. *Astrometriya: Astrofizika, 1, Fizika Luny: Planet*, Kiev, Naukova Dumka Press 1968), NASA-Technical Translation-F-566, 33-45.

The profiles of 29 craters on the far side of the Moon are reviewed. The photographs obtained by the automatic interplanetary station Zond 3 were used. The photometric method of investigating the lunar surface was applied, and the method of obtaining the profiles of craters from lunar photographs taken from a spacecraft is described. The size and form of the lunar craters on the far side are similar to those on the near side. The depth-to-diameter ratios obtained for the craters under investigation are the same as those assumed for the eruptive craters. The older craters have greater dimensions and depths. Younger craters possess conical inner slopes.

Mironova, M. N.: 'Height Profiles of Twenty-nine Craters on the Far Side of the Moon', in *Astronomy and Astrophysics*, No. 1: *Physics of the Moon and Planets* (ed. by I. K. Koval – Transl. into English of the Publ. *Astrometriya: Astrofizika, 1, Fizika Luny: Planet*, Kiev, Naukova Dumka Press 1968), NASA-Technical Translation-F-566, 46-57.

The profiles of 29 craters on the far side of the Moon are shown. The photometric method was used in obtaining these crater profiles. An analysis of the results is given.

Ronca, L. B. and Green, R. R.: 'Statistical Geomorphology of the Lunar Surface', *Geol. Soc. Am. Bull.* **81**, 337-352.

When the lunar crater area density (number of craters per unit area) is contoured on the lunar surface, it is evident that lunar craters are not distributed at random. The terra-mare dichotomy is clearly indicated and, in addition, the terrae themselves display nesting and parallelism of the contours. A

mathematical 'nesting index' is defined, which varies from zero for a random set of contours to 1 for a perfect bull's eye. For the whole front face of the Moon, the nesting index is as high as 0.90. When only the southern terrae are considered, the nesting index is as high as 0.83. Also, there are systematic relationships between the classes of craters (degree of erosion) and crater density. As a result of these observations, the following working hypothesis is proposed. Two independent erosional processes operate on the lunar surface. The first is continuous and reduces craters from class 1 to class 2 to finally class 3 and sometimes class 4. The second process is discontinuous and produces craters of class 5 and occasionally class 4. Barring interference from the discontinuous process, a newly formed crater will remain in class 1 for the length of time necessary for the crater density of that area to increase by a value, k . In practice k ranges from 6 to 24 craters per 58×10^8 km². It can be shown that such a process is described by a line of slope -1 when the logarithm of the percentage of class 1 craters is plotted versus the logarithm of the density of craters. The position along this line of slope -1 of any lunar area is defined as the geomorphic index. The distribution and location of this index suggest the presence of two types of processes of rejuvenation on the lunar surface. The first, and most evident, is mare flooding, which is able to completely bury the majority of craters of an area or reduce them to class 4 or 5. For the case of the maria it is likely that the geomorphologic indices are closely related to time indicates, that is, geomorphologically younger maria were the most recent to be formed. The probable order of formation of the mare surfaces is presented. The second process of rejuvenation operated on the terrae. It can be shown that rejuvenation progressively decreases as one goes from a mare shore toward the center of the terrae. The hypothesis is presented that mare-producing impacts rejuvenate the environs of the impact locus by seismic waves and ballistic sedimentation. Rejuvenation can also explain the nesting indices of the crater density contours, previously described.

Russell, J. A. and Mayo, M. J.: 'A Comparison of the Frequency Size Distribution of Martian 'Oases' with Those of Lunar Craters and of Martian Craters', *Meteoritics* 4, 293.

Since the successful flight of Mariner IV, Öpik and Tombaugh have independently reiterated their earlier belief that Martian oases are impact craters. The correctness of their surmise may soon be definitely established or refuted by data from the probes presently approaching Mars. In this paper, evidence based on the study of Earth-based observations is presented in support of their theory. Counts and diameter determinations of oases were made by both authors, using three well-known maps of Mars. Intentionally, there was no discussion of the basis for measuring the diameters or choosing the objects to be included previous to the measuring. The data were arranged so that they could be added to a Log Cumulative Number per 10^6 square kilometers vs Log Diameter plot published by Leighton, in which he included curves for craters on lunar maria, craters on lunar highlands, and craters on Mars, as revealed by the Mariner IV data. Plots for all three maps fell on lines closely parallel to those of Leighton and lying between his curves for Martian craters and for craters on the lunar maria. Hence, fewer oases were observed than expected on the assumption that they are a continuation of the Martian crater population in the direction of larger objects. This suggests the presence of an incompleteness factor such as the visibility of only the more recently formed craters. By the time that it is presented, this paper will be little more than a historical note. It may indicate, however, that Lowell and Slipher saw more on Mars than all gave them credit for, or it may merely indicate the fallibility of the human machine as a data recorder. (Abstract only.)

Trask, N. J.: 'Ranger Photographs of the Moon', *Radio Sci.* 5, 123-128.

Photographs from the Ranger probes provided the first direct evidence on the fine-scale topography of the Moon and showed that the surface is relatively smooth over slope distances of 1 meter. In addition to craters, elements contributing to the topography at this scale are the closely spaced ridges and troughs of lunar patterned ground. Blocks in the size range 0.5 meters to several meters were not seen in the Ranger pictures, perhaps because of the limited sampling at three widely separated points. Ranger-7 photographs showed the preponderance of shallow elongate to circular craters along rays. Ranger-8 photographs were notable for portraying with new clarity the craters Sabine and Ritter, which appear to be of internal rather than impact origin. Ranger-9 photographs of the floor of the crater Alphonsus contained data from which a complicated geologic history of the floor can be deciphered.

Tyler, G. L. and Simpson, R. A.: 'Bistatic Radar Measurements of Topographic Variations in Lunar Surface Slopes with Explorer-35', *Radio Sci.* **5**, 263–271.

Bistatic radar observations of the lunar surface conducted with Explorer-35 at 2.2 meters have been used to measure the average large-scale (tens to hundreds of meters) lunar slopes. Data obtained for the equatorial band between 70° east and west longitude show significant (3:1) regional variations. Unidirectional rms slopes of 2°, 3°, and 6° were obtained for Mare Fecunditatis and Oceanus Procellarum the central highlands and terra surrounding the crater Alfraganus, and the Censorinus highlands, respectively. A comparison of the slope variations and visible surface structure suggests that the meter wavelength radar slopes are those of the visible surface measured on the set of scales given above.

10. Origin and Stratigraphy of Lunar Formations

Baldwin, R. B.: 'Absolute Ages of the Lunar Maria and Large Craters', *Icarus* **11**, 320–331.

By an analysis of the changes in rim heights of lunar craters through isostatic settling, combined with inferences from counts of small impact craters contained within and subsequent to large craters, it is concluded that: (1) the maria are not older than about 640 million years – and (2) the flux of masses which produced craters larger than 160 km in diameter reached a peak rate at a maximum age of about 2.5 billion years ago, and not very early in the Moon's history as has usually been thought.

Blodget, H. D., Lowman, P. D., Jr., and O'Keefe, J. A.: 'Geologic Analyses of Selected Apollo-10 70 mm Lunar and Terrestrial Photographs', NASA-Technical Memorandum-X-63925; X-644-70-165.

Geologic analyses of selected Apollo-10 70 mm photographs taken during translunar coast, lunar orbit, and transearth coast are presented. Photographs of sinuous and nonsinuous rilles in Mare Tranquillitatis and north-eastern Sinus Medii reveal X-shaped intersections and segments of rilles crossing hills, suggesting a basically tectonic rather than fluid flow origin. Detailed photographs of highland craters on the Moon's far side show mass wasting that appears to have occurred by continuous flow, rather than in discrete slump blocks, which indicates a deep noncohesive fragmental layer for such areas. Other photographs show mare ridges capped by higher albedo hills that are apparently younger than the ridges, and which are thus suggested to be volcanic extrusions from the ridges. Several nearly vertical photographs of Mare Smythii taken with high Sun angles show dark centered craters with bright walls, which may be of internal origin. The color of the Earth's surface can be seen with relatively little atmospheric distortion from distances of 30000 miles or more, and enables recognition of a great amount of topographic detail in North Africa, southwest Asia, and North America. Brief descriptions of the major physiographic features visible on selected Earth photographs are presented.

Ehmann, W. D. and Morgan, J. W.: 'Twin Terrestrial Impact Craters', *Nature* **225**, 255.

Mills has suggested that certain multiple or twin lunar craters may have formed by the slow collapse of a fluidized bed and has noted that violent events forming craters, such as meteorite impacts, would be expected to cause considerable destruction of the dividing wall in multiple craters. The authors point out that a terrestrial example of multiple impact craters with dividing walls essentially retained does exist in the Henbury meteorite crater group in Central Australia. This three crater grouping has many features similar to the multiple lunar craters discussed by Mills and is clearly due to meteorite impact.

El-Baz, F.: 'Lunar Igneous Intrusions', *Science* **167**, 49–50.

Photographs taken from Apollo-10 and -11 reveal a number of probable igneous intrusions, including

three probable dikes that crosscut the wall and floor of an unnamed 75-kilometer crater on the lunar farside. These intrusions are distinguished by their setting, textures, structures, and brightness relative to the surrounding materials. Recognition of these probable igneous intrusions in the lunar highlands supports the indications of the heterogeneity of lunar materials and the plausibility of intrusive igneous activity, in addition to extrusive volcanism, on the Moon.

Elder, J. W.: 'Lunar Continental Migration and Maria Spreading', *Nature* **225**, 842-844.

This report considers the possibility that the lunar maria were formed by internal geological processes similar to those which formed the ocean floors of the Earth. The early stages of the cooling of all bodies of planetary size is the same, provided the initial temperatures and the rock types are similar. Vigorous convection is confined largely to a thin sublayer near the surface and the interior of the body is little affected. The lunar evidence suggests that mare production arising from vigorous penetrative convection is the dominant process at this stage. Gradually the internal energy of the body becomes depleted and if the body is sufficiently small, as seems to be the case with the Moon, convective processes rapidly lose their vigour and the mare structure is 'frozen'.

Erlich, E. N., Gorshkov, G. S., Melekestsev, I. V., and Steinberg, G. S.: 'The Structure of the Lunar Crater Tsiolkovsky', *Modern Geol.* **1**, 197-201.

An impact origin of the crater Tsiolkovsky is refuted for the following reasons: (1) Lava flooding on the crater floor occurred during more than one effusive phase. (2) The central peak shows varying degrees of erosion. (3) There is no circular symmetry of the explosive deposits. (4) Areal crater densities are not related to the age of the respective surface. (5) The appearance of the surface of some of the deposits is similar to the surface of pyroclastic flows which were heavily saturated with gas.

Fudali, R. F. and Melson, W. G.: 'Secondary Craters as a Clue to Primary Crater Origin on the Moon', *Meteoritics* **4**, 273.

During the explosive phase of the Volcan Arenal (Costa Rica) eruption in July, 1968, ejected blocks were thrown as far as 5.5 kilometers from the explosion crater opened on the west flank of the volcano. These blocks created an extensive field of secondary craters, the largest of which was 30 meters in diameter. Chamber pressure just prior to the eruption must have been about 900 atmospheres, based on calculated ejection velocities of 250 m/sec. Ejection velocities and pressures in this range are not excessive and are probably not unusual in the initial phases of explosive, terrestrial volcanic activity. The diameter of the explosion crater itself is only about 100 meters so that numerous secondary craters were formed at distances corresponding to greater than 100 crater radii. On the Moon, all else being equal, these secondary craters would have been formed out to more than 30 kilometers or 600 crater radii from the volcano. By way of contrast the Sedan nuclear event, often used as a model to illustrate meteorite impact phenomena, threw ejecta a maximum of 20 crater radii, with most of the ejecta being confined to 10 crater radii. The lunar surface is heavily pockmarked with craters and our understanding of its history must depend upon our ability to correctly interpret the origins of these circular features - using only altitude photography and minimum 'ground truth' information. Many astrogeologists currently feel that extended secondary crater fields and the presence of 'base surge' deposits are diagnostic of primary lunar impact craters. Based on the evidence presented here we suggest that the extent of secondary crater fields has little value as a criteria of impact. The case for 'base surge' deposits should also be viewed with some suspicion.

Gault, D. E.: 'Saturation and Equilibrium Conditions for Impact Cratering on the Lunar Surface: Criteria and Implications', *Radio Sci.* **5**, 273-291.

A model based on first principles and laboratory results is presented for describing and evaluating long term effects of meteoritic impact against the lunar surface. The evolution of the cratered surface and concomitant regolith is calculated and compared with observations and analyses of Lunar Orbiter

photographs. It is indicated that most craters are of impact origin, but gross differences in the apparent ages of surfaces in various units and regions of the Moon imply that endogenic processes also must have been active, probably since the beginning of Precambrian time and, perhaps, as recently as a few million years ago.

Gilvarry, J. J.: 'The Origin and Nature of Lunar Mascons', *Radio Sci.* **5**, 313-323.

The origin of the mascons is explained in terms of a primordial atmosphere and hydrosphere of the Moon lasting of the order of 1 b.y. from the origin of 4.5 b.y. ago. On this basis, the mascons arose in four steps: (1) excavation of a large crater by meteoritic impact at a time close to the Moon's origin, (2) subsequent isostatic adjustment of its rim and true floor, (3) rigidification of the crater and extensive deposition of sediments in its interior while an atmosphere and hydrosphere existed, and (4) eventual desiccation of the sediments in the floor when the atmosphere and hydrosphere vanished. Rigidification of the crater (within a time about 1 m.y. after the Moon's origin) prior to the main deposition of the sediments implies that the mascon load is supported by the strength of the underlying rock to produce a positive gravitational anomaly (independently of sediment density).

Greely, R.: 'Terrestrial Analogs to Lunar Dimple (Drainage) Craters', *Meteoritics* **4**, 276.

Some lunar craters have been described as resulting from drainage of fragmental surface material into subsurface cavities, or withdrawal (drainage) of magma beneath a plastic lava crust; these features are termed drainage craters, characterized by their: (1) lack of raised rim; (2) convex-up slope; (3) small diameter; (4) often elongate form in planimetric view; (5) association often with similar craters in crater chains (some crater chains are aligned with regional structural trends); and (6) steeper slopes toward the center than near the periphery (dimple crater *sensu stricto*). Dimple craters are considered a special form of drainage crater characterized by the central 'dimple' shaped depression. In addition to modes of formation offered by previous investigators, terrestrial drainage craters formed over lava tubes in Oregon are presented as analogs to lunar drainage craters. Craters associated with lava tubes result from: (1) drainage of surface material through roof fractures; (2) plastic collapse of the partially cooled lava tube roof; and (3) drainage of surface material into roof collapses. The former categories result in shallow, often elongate craters; the latter category forms classic 'dimple' shaped craters. Elongate dimple craters formed over volcanic fissures in southern Idaho are also discussed and presented in support of one mode of formation proposed by previous investigators for lunar drainage craters. Movement of surface material toward the orifice is initiated on Earth largely by wind and water; in lunar conditions initial movement is attributed to micro and macrometeoritic bombardment, seismic disturbances generated by internal and external processes, and by thermal creep.

Grine, D. R.: 'Bed Forms in Base-surge Deposits: Lunar Implications', *Science* **167**, 1637-1638.

The author points out that lunar surface features which have been described by Fisher and Waters (1969) as bed forms of sedimentary deposits cannot at this time be considered formed by a base surge mechanism. Base surges of meteor craters and volcanoes cannot exist without the presence of an atmosphere.

In a following letter, Fisher and Waters suggest that base-surges could develop near craters on the Moon, despite the absence of an atmosphere. Large impacting meteorites could produce sufficient vapor to create temporary gaseous 'atmospheres' in which particles could be entrained and perhaps move farther than clouds of comparable size on the Earth.

Hapke, B. and Greenspan, B.: 'Crater Densities in the Vicinity of Lunar Sinuous Rills', *EOS* **51**, 346.

Crater densities in the 0.1-1 km size range were measured in the vicinity of 4 lunar sinuous rills using Lunar Orbiter pictures. Densities are significantly greater on the floors of 3 of the rills than on the adjacent maria. Densities in the 4th rill are lower than on the surrounding mare, but the region appears

to have been heavily cratered by secondary ejecta from Aristarchus. This data argues against those hypotheses for the origin of sinuous rills by simple down-cutting by a moving fluid. (Abstract of a paper presented at the April 1970 meeting of the American Geophysical Union.)

Hartmann, W. K.: 'Preliminary Note on Lunar Cratering Rates and Absolute Time-Scales', *Icarus* **12**, 131–133.

Solidification ages from Mare Tranquillitatis (Apollo-11) are used to compute the lunar cratering rate over the last 3.9 aeons. Results agree with estimates from more recent terrestrial cratering.

Howard, A. D. and Rich, E. I.: 'Lunar Analogs of Fluvial Landscapes: Possible Implications', NASA-Contractor's Report-109842.

Geomorphic approach to the problem of whether any features of the lunar landscape require fluid erosion is presented. The sculpturing of the lunar highlands suggests fluid erosion at an early stage in lunar history. The post-mare meandering rilles are sparsely distributed and largely confined to the lunar maria. Localized fluid erosion is also suggested by terrestrial-type valleys on the inner and outer flanks of both pre- and post-mare craters.

Howard, K. A.: 'Mascons, Mare rock and Isostasy', *Nature* **226**, 924–925.

The author proposes that before mare flooding the lunar rigidity was much less than after, so that considerable isostatic adjustment was possible before but not after. This sequence is suggested by a contrast in morphology between young and old craters. Some of the large impact basins are old enough so that, by the time flooding started, substantial isostatic levelling would have already occurred. As a result, only a thin layer of mare material was deposited in these old basins. Younger basins had not yet reached equilibrium and were still deep by the time flooding started, so they were filled with a great thickness of mare material, in excess of the amount that would be isostatically balanced. By this time, the outer part of the Moon had cooled to a more rigid state so that isostatic adjustment could not take place. The Oceanus Procellarum area may represent not merely volcanic flooding into a crustal scar as in the case of the circular basins but a major centre of high heat flow.

Hubbard, J. H. and Gall, E. S.: 'Lunar Soil Simulant Study, Phase B. Part 1: Outgassing Characteristics; Final Report', Ohio River Div. Labs. Technical-Report-4-58.

The work describes an investigation of the outgassing characteristics of diabase rock crushed to a gradation equivalent to a fine sand. Materials were heated in air to various temperatures and for several exposure periods and were then placed in a high vacuum chamber for pump down. The variation of pressure with time was plotted and the effect of nitrogen overlays between successive pump downs were evaluated. The one-dimension diffusion equation was solved to indicate the way in which pressure varies with depth.

McCall, G. J. H.: 'Lunar Rilles and a Possible Terrestrial Analogue', *Nature* **225**, 714–716.

The author concludes that Sinuous Rilles are not water scouring patterns, nor are they products of lateral scouring by fluidized systems akin to ash-flows. They are volcano-tectonic fracture traces which are sites of gas emission.

Novikov, V. V.: 'The Structure and Proposed Composition of Rocks on the Floors of Young Lunar Craters', *Soviet Astron. – AJ* **13**, 874–877.

Morphological analogs for several lunar formations in the Kamchatka volcanic region are presented. The results obtained by the author during the 1967 Kamchatka expedition are used to compare the

relative spectral brightness distribution of sunlight at wavelengths up to 2.5μ for volcanic deposits and for certain areas on the Moon. It is concluded that lava flows more acid in composition than basaltic slag occur on the floors of young lunar craters.

Oberbeck, V. R., Quaide, W. L., and Greeley, R.: 'On the Origin of Lunar Sinuous Rilles', *Modern Geol.* **1**, 75–80.

Sinuous rilles on the lunar surface have morphologic features indicative of an origin through fluid flow. Evidence is presented which suggests that the fluid can be lava and that some smaller sinuous rilles may have been formed by collapse of lava tubes.

Schubert, G., Lingenfelter, R. E., and Peale, S. J.: 'The Morphology, Distribution, and Origin of Lunar Sinuous Rilles', *Rev. Geophys. Space Phys.* **8**, 199–224.

The selenographic locations and measurements of such morphological characteristics as length, width, meander wavelength, and minimum average depth have been obtained for about 130 lunar sinuous rilles. We conclude that the morphology of the sinuous rilles requires that they be features of surface water erosion, which could occur in the present lunar environment, since a layer of ice can pressurize the water and maintain it in a liquid phase. Water is assumed to be trapped beneath a permafrost layer, which is shown to be stable on a geologic time scale. The concentration of the rilles around the circular basins and craters and associates the outgassing of the lunar interior with major impacts. The rille meander pattern is characterized by a median wavelength to width ratio > 4 , a value not inconsistent with ratios found for terrestrial alluvial rivers. The generally smaller ratio of meander wavelength to width for lunar sinuous rilles than for terrestrial rivers may indicate that the lunar rivers responsible for eroding the rilles transported a larger percentage of suspended-load material than is carried by terrestrial rivers. We estimate that the amount of water ultimately available on the lunar surface is two orders of magnitude greater than that required to erode all the sinuous rilles. This estimate of the available water is in agreement with the measured water content of the Apollo-11 lunar samples.

Seeger, C. R.: 'A Geological Criterion Applied to Lunar Orbiter-5 Photographs', *Modern Geol.* **1**, 203–210.

A geological criterion of origin, i.e., the present position of rocks in crater rims and walls for which a position prior to the cratering event can be deduced, has been applied to Lunar Orbiter-5 photographs. Terrestrial volcanic craters and maars have flat-lying rocks in the walls at lower levels than the surrounding terrain and undeformed depositional rims. Impact craters have deformed rocks in the walls exposed at levels above the surrounding terrain and deformational rims with the rocks quaquaversal. When this difference was applied to the Lunar Orbiter-5 photographs, numerous examples of each kind were found. Thus both major processes suggested for lunar cratering (endogenetic and exogenetic) have been operative.

Short, N. M.: 'Thickness of Impact Crater Ejecta on the Lunar Surface', *EOS* **51**, 346.

Calculations based on improved models for impact cratering indicate an average thickness (spread uniformly) of ejecta from craters larger than 10 km on the visible face of the Moon that ranges from 0.48 km to 2.75 km depending on combinations of critical parameters. These parameters include: 1) initial effective diameters, 2) depth/diameter ratios between 0.05-0.30, 3) fractional enlargement of diameters by slumping (up to 0.5), 4) efficiency of ejection, 5) frequency distribution of craters in various size classes, and 6) appropriate selection of circular structures as impact-generated. Chief uncertainty is the identification of those large basins directly caused by impact; where mare-filled, the proper choice of diameter becomes critical. Contributions from mascon-related basins vs all roughly circular basins are considered. The apparent thickness of rubble cover ($\sim 1-10$ m) on some mare surfaces implies that most major craters were formed early in lunar history, followed by lava extrusion. An anorthositic lunar highlands (suggested by Apollo-11 results) should be variably covered by ejecta derived largely from impact basins penetrating a pre-mare crust (anorthosite?). If

the Moon's outer mantle initially was built up by accretion, ejecta from earlier (now covered) craters would add to the average thickness from observable craters. (Abstract of a paper presented at the April 1970 meeting of the American Geophysical Union.)

Smith, E. I.: 'The Determination of Origin of Small Lunar and Terrestrial Craters by Depth-Diameter Ratio', *EOS* **51**, 342.

Measurements of 140 small (< 3.5 km diameter) terrestrial meteorite impact and volcanic craters show consistent differences in ratios of depth (d) to diameter (D). A plot of $\log D$ vs $\log d$ indicates two distinct fields, volcanic (high d/D) and impact (low d/D) separated by Baldwin's 0.50 scaled depth-of-burst curve. A plot of 170 small lunar craters indicates differentiation into the same fields. Randomly distributed, ray and bright halo craters fall into the field of terrestrial impact craters, whereas summit pits of domes and cones (e.g., Rümker Hills, Marius Hills) fall into the field of terrestrial volcanic craters. The fields converge for values of $D \lesssim 4$ km and $d \lesssim 400$ m. This depth-diameter relationship is being used to identify lunar volcanic and impact morphologies. Over 50 previously unreported lunar cratered volcanic domes and cones have been recognized using this technique as a criterion for identification. Lunar crater depths were determined by shadow method and from Ranger Lunar Charts. (Abstract of a paper presented at the April 1970 meeting of the American Geophysical Union.)

Soderblom, L. A.: 'A Model for Small-impact Erosion Applied to the Lunar Surface', *J. Geophys. Res.* **75**, 2655–2661.

A model for erosion of the lunar surface by impact of small projectiles is developed that provides an analytic representation of the change of crater shape as a function of time. The model is applied to the erosion of craters approximately 1 m to 1 km in diameter. The lifetime of a crater in this size range, which is steadily eroded by impact, is approximately proportional to its radius. The model predicts the observed steady-state size frequency distribution of small lunar craters and the dependence of this distribution on the crater-production curve.

Wegener, A.: 'The Origin of the Lunar Craters', NASA-Contractor's Report-109327.

Wise, D. U. and Yates, M. T.: 'Mascons as Structural Relief on a Lunar Moho', NASA-Contractor's Report-109768; Technical Report-70-340-2.

A mechanism for the creation of lunar mascons is proposed that requires no abnormal density materials nor density inversions. The mascons are produced by mantle plugs upwelling into giant impact basins punched through the lunar crust followed by volcanic filling of the remainder of the crater above the plug. It is explicitly shown that continued volcanic filling is not inhibited by the attainment of isostatic equilibrium. This model predicts a minimum crystal depth of 45 km in the Imbrium region, assuming a 0.5 g/cm^3 density contrast between the lunar crust and mantle. The strength of the lunar mantle must be somewhat greater than the Earth's, however, this is not inconsistent with a composition essentially similar to the Earth's. The approximate linear relationship between the peak gravity anomaly and the mare basin diameter suggests that for craters less than 200 km diameter, the strength of the Moon is sufficient to prohibit the formation of a mascon by mantle upwelling and volcanic filling.

11. Physical Structure of the Lunar Surface

Bader, H.: 'The Hyperbolic Distribution of Particle Sizes', *J. Geophys. Res.* **75**, 2822–2830.

Many natural collections of small particles, such as cosmic and terrestrial dust, mineral and organic particles suspended in sea water, and fine sediments, have a size distribution well formulated by the

equation $N = Kx^{-c}$, where N is the number of particles larger than size x and K and c are constants. A number of equations are derived for calculating the interesting parameters characterizing hyperbolic distribution, which are illustrated by new Coulter Counter measurements of dust and sea water. An appendix lists useful equations, generalized for different size parameters.

Christensen, E. M.: 'Lunar Surface Mechanical Properties: Surveyor Results', *Radio Sci.* **5**, 171–180.

Lunar surface mechanical properties have been interpreted from the interactions of five Surveyor spacecraft with the lunar surface (exclusive of the surface sampler). The lunar soil at the one highland and the four lunar mare landing sites is remarkably similar, even though these sites are widely separated. The soil is predominantly fine-grained and granular; it is estimated to have a cohesion value between 0.05 and 0.17 N/cm². The static bearing strength of the soil increases with depth. It is estimated that, at the surface, the strength is less than 0.1 N/cm²; at a depth of 4 cm, for a 25-cm diameter plate, the strength is somewhat greater than the originally estimated 4 to 6 N/cm². The soil, at least in the upper few centimeters, is compressible.

Greenwood, W. R. and Heiken, G.: 'Origin of Glass Deposits in Lunar Craters', *Science* **168**, 610–611.

In a reply to Gold's suggested explanation for certain glass deposits in small lunar craters, the authors describe photographs of such deposits in greater detail, and offer support for a different hypothesis of formation. The glass spheres, pancakes, and rock coatings appear to be rock and lunar surface material fused by meteorite-impact explosions that excavated the craters in which the largest amount of the glass has been observed. The material under and around the crater was probably indurated by the shock wave from the explosion. The glass deposited as fallback from the explosion and therefore coats the prominent features of the indured crater bottom. Loose material thrown out by the explosion covers crater walls and rims and slumps into craters, tending to cover the glass deposits. Some small rocks became either partly or entirely glass-coated while in the explosion plumes above craters.

Hagfors, T.: 'Remote Probing of the Moon by Infrared and Microwave Emissions and by Radar', *Radio Sci.* **5**, 189–227.

The results of the remote probing of the Moon by means of infrared and microwave emissions and by radar are reviewed. Also, we discuss how the various observational results can help to explain physical parameters of the lunar surface, such as thermal and electrical conductivities, dielectric constant, density, particle sized in the lunar regolith, depth of the surface layer, roughness of the surface, variation of these parameters from point to point on the surface, and amount of heat generated in the lunar interior.

Marcus, A. H.: 'Interpretation of Lunar Rock Size Distributions', *EOS* **51**, 346.

Combining local size distributions into a single size distribution for a large area is not justified because different local distributions correspond to different physical processes. Most of the observed exponents of the inverse-power distributions in small regions are very close to one of the values $s = 2.6$ or $a = 1.6$; a few places have $s = 2.0$. Freshly formed rocks, either excavated from bedrock or aggregated from regolith by meteoroid impacts, have $s = 2.6$. An old population of hard rocks repeatedly split by impacts has $s = 2.0$. $s = 1.6$ may represent eroded soft aggregates, but for small rocks is more likely due to burial. Surface rocks evolve by catastrophic splitting, erosion, burial and uncovering. Splitting may be dominant for large rocks since there are virtually no large 'ghost rocks' produced by erosion or burial. If the Moon is losing mass by meteoroid impact, fine particles are preferentially removed from the top layer and larger rocks uncovered, decreasing the observed value of s . Volume distributions thus cannot be directly estimated from surface counts. Some surface counts in regions distant from the camera appear to be observationally incomplete. (Abstract of a paper presented at the April 1970 meeting of the American Geophysical Union.)

Mason, C. C.: 'Nature of the Martian Surface Layer as Inferred from the Particle Size Distribution of Lunar Surface Materials', *EOS* **51**, 343.

The Apollo-11 core sample tubes were 2 cm in diameter, so particles > 2 cm were excluded from the samples. The percentage of > 2 cm particles from the Surveyor-1 particle count data was added to the Apollo-11 data and the data normalized. When plotted as a log normal distribution, the Surveyor-1 curve joins the core 1 and core 2 curves smoothly. There is a sharp break in the size distribution curve which can be explained by the material actually being composed of two populations, one population due to comminution from the impact of the larger sized meteorites and the other population due to the melting of fine material by the impact of smaller sized meteorites. The Martian atmosphere will volatilize the smaller incoming meteorites. It will slow down incoming meteorites of intermediate and large size, causing comminution and stirring up the particulate layer. The combination of comminution and stirring up of material will result in prevailing winds of the Martian atmosphere sorting out the very finest material and transporting it to regions of calm where it will be deposited. As a result, the Martian surface in the region of prevailing winds should consist of a fine-grained desert pavement, and the regions of calm and shifting winds should consist of extremely fine-grained sand dunes. (Abstract of a paper presented at the April 1970 meeting of the American Geophysical Union.)

Mason, C. C.: 'Comparison of Actual Versus Predicted Lunar Surface Erosion Caused by Apollo-11 Descent Engine', *Geol. Soc. Am. Bull.* **81**, 1807-1812.

The Apollo-11 lunar module landed with an estimated 2 ft/sec lateral motion. Photographic evidence and astronaut observations indicate that only a fraction of an inch of material was eroded from the surface during the descent. These indications agree with a computed maximum depth of eroded material using an empirically derived erosion law. The onset of erosion was determined from descent motion pictures and astronaut comments during the landing approach. The first noticeable erosion occurred when the lunar module was at 65 ft, followed by thin steady erosion at 55 ft and strong steady erosion at 45 ft. These observations compare with a predicted onset of erosion at greater than 40 ft and fully developed erosion between 20 and 40 ft.

Mitchell, J. K., Carmichael, I. S. E., Goodman, R. E., Frish, P., and Witherspoon, P. A.: 'Material Studies Related to Lunar Surface Exploration. 4: Preliminary Studies for the Design of Engineering Probes', NASA-Contractor's Report-107173.

Mitchell, J. K., Carmichael, I. S. E., Goodman, R. E., Frisch, J., and Witherspoon, P. A.: 'Material Studies Related to Lunar Surface Exploration', NASA-Contractor's Report-107174.

Mitchell, J. K., Carmichael, I. S. E., Goodman, R. E., Frisch, J., and Witherspoon, P. A.: 'Material Studies Related to Lunar Surface Exploration, 2: Application of Geophysical and Geotechnical Methods to Lunar Sites Exploration', NASA-Contractor's Report-107175.

Murase, Tsutomu and McBirney, A. R.: 'Viscosity of Lunar Lavas', *Science* **167**, 1491-1493.

The viscosity of a synthetic silicate liquid with the composition of a lunar rock has been determined experimentally and found to be lower than that of any previously studied volcanic rock on Earth. This fact suggests that lunar lava flows will be very thin and extensive unless they are ponded, and that lava tubes should be common and of larger dimensions than those on Earth. Coarse crystallinity can be a feature of rapidly cooled surface lavas.

Neukum, G., Mehl, A., Fechtig, H., and Zähringer, J.: 'Impact Phenomena of Micro-meteorites on Lunar Surface Material', *Earth Planetary Sci. Letters* **8**, 31-35.

The NASA lunar surface samples 10019 and 10046 from the Apollo-11 mission were searched for

micrometeorite impact craters by means of an optical reflecting microscope and a Stereoscan electron microscope. Craters with diameters between 2 microns and 0.8 mm were observed. Approx. 1 crater larger than 0.15 mm in diameter per 1 mm² and 1 crater larger than 2 μm per 500 μm² could be found. The time of exposure is calculated from crater number densities and cosmic dust influx values to be 10000 yr and 100 yr for layers of respective thicknesses. On lunar glassy spherules impact features were found which yield the same crater number densities. The phenomenology of high velocity impacts was studied by shooting microspheres on targets similar to lunar material using a 2 MV dust accelerator.

Schreiber, E. and Anderson, O. L.: 'Properties and Composition of Lunar Materials: Earth Analogies', *Science* **168**, 1579–1580.

The sound velocity data for the lunar rocks were compared to numerous terrestrial rock types and were found to deviate widely from them. A group of terrestrial materials were found which have velocities comparable to those of the lunar rocks, but they do obey velocity-density relations proposed for Earth rocks.

Shoemaker, E. M. and Morris, E. C.: 'Physical Characteristics of the Lunar Regolith Determined from Surveyor Television Observations', *Radio Sci.* **5**, 129–155.

The new data on the physical characteristics of the lunar surface derived from the Surveyor pictures can be fitted to a simple ballistic model for the origin and development of the lunar regolith. The thickness of the lunar regolith may be estimated from a variety of observational data. The estimated thickness of the regolith at a given Surveyor landing site is bracketed by the original depths of (1) the smallest blocky-rimmed craters that cut through the regolith and excavate coherent material beneath, and (2) the largest, sharp, raised-rim craters without blocks that have been excavated wholly within the slightly cohesive material that forms the regolith. Other direct estimates of the thickness of the regolith are the inferred original depth of the largest craters believed to have been formed by drainage of the regolith material into subregolith fissures and, at the Surveyor-7 site, the depth at which the surface sampler instrument encountered coherent material. The thickest regolith was found at the Surveyor-6 site, where it is estimated to be more than 10 m thick, and the thinnest was found at the Surveyor-7 site, where it is estimated to be 2 to 15 cm thick. Particle counts from sample areas at each of the Surveyor landing sites show an approximately linear relationship between the log of the cumulative particle counts and the log of the particle size. A power function of the form $N = KD^{\lambda}$ (where N is the cumulative number of particles with diameter equal to or larger than D , and D is the diameter of particles) can be fitted to the data at each site. The size-frequency distribution of resolvable fragments at the Surveyor 3, 5, and 6 landing sites was found to be the same, within errors of estimation, but at the Surveyor 1 and 7 sites coarse fragments are more numerous. Considering all five sites, we found a strong inverse correlation between the abundance of coarse blocks and the thickness of the regolith. The coarsest fragments are most abundant at the sites with the thinnest regolith.

Soga, N. and Anderson, O. L.: 'Some Physical Properties of the Lunar and Artificial Glasses', *EOS* **51**, 347.

Sound velocities and Poisson's ratio of glass spheres from the lunar soil (300–600 micron diameter) were measured using the resonant sphere technique. The sound velocities were found to be almost constant ($v_p = 6.3$ – 6.5 km/sec; $v_s = 3.5$ – 3.7 km/sec) in spite of large variation in density (2.8–3.2), whereas Poisson's ratio increases almost linearly with density. Both of these results are attributable to the increase in Fe and Ti, which is consistent with the results of artificial glasses with lunar materials – like compositions. The data were also used to estimate the sound velocities of parent lunar rocks by means of the fourth-power relationship between the elastic moduli and the density for the glassy and crystalline materials. The results agree reasonably well with the data obtained on the lunar rocks. (Abstract of a paper presented at the April 1970 meeting of the American Geophysical Union.)

Strick, E.: 'Anelasticity and the Apollo-12 LP Lunar Seismogram', *Earth Planetary Sci. Letters* **8**, 234-236.

Further refined arguments are given to support the author's low- Q regolith layer model as deduced from the Apollo-12 LP seismogram. It is also shown that this model can yield the same response envelope as does a high- Q model based upon the diffusion equation that has been suggested by Latham *et al.*

Strick, E.: 'Anelasticity and Lunar Seismology', *EOS* **51**, 363.

Derived relations from the author's power-law model for the anelastic behavior of sedimentary earth rock are presented for possible use in understanding the long-time response behavior of lunar seismograms. As an illustrative example of the use of these relations we have shown how they can be used together with parameters determined from field experiments by De Bremaecker, Godson and Watkins in basaltic cinders and ash near Flagstaff, Arizona to yield reported properties of the seismogram obtained in the Apollo-12 experiment. The long tail is predicted to be due to overlapping of P -wave multiples in a regolith layer where each of the multiples has undergone a pulse broadening of between 7 and 9 min for the 75 km travel distance. The P -wave velocity of the regolith seems to be about 300 m/sec and the thickness perhaps 300 m. These values are subject to change after the author has had an opportunity to examine the Apollo-12 seismogram. (Abstract of a paper presented at the April 1970 meeting of the American Geophysical Union.)

Thompson, T. W., Pollack, J. B., Campbell, M. J., and O'Leary, B. T.: 'Radar Maps of the Moon at 70-cm Wavelength and their Interpretation', *Radio Sci.* **5**, 253-262.

Polarized and depolarized radar maps of the Moon have been obtained at the Arecibo Ionospheric Observatory at a wavelength of 70 cm. These maps show strong positive anomalies, many of which are associated with young craters. These anomalies and the average diffuse component of radar echoes are attributed to the scattering behavior of surface and subsurface rocks. We have been able to approximately match the observed spatial and wavelength variation of the diffuse component, as well as the absolute value of its cross section, with theoretical calculations that use a Mie scattering description of the single scattering behavior of the rocks, and to employ the Surveyor spacecraft's determination of the size distribution of surface rocks. Furthermore, we have found that surface rocks appear capable of accounting for temperature anomalies (IR hot spots) which are associated with these craters.

Tikhonova, T. V. and Troitskii, V. S.: 'The Spectral Reflection Coefficient of the Lunar Surface for Radio Waves, and the Depth Dependence of the Soil Properties', *Soviet Phys. - Astron.* **13**, 1039-1043.

The spectral power reflection coefficient is determined for two models of the lunar surface layer by solving the Riccati equation on a digital computer. Comparison with experiment indicates that both models adequately explain the radar curve for the reflection coefficient. The estimate $a_2 = 200 \pm 100$ cm is obtained for the thickness of the porous layer.

Tolansky, S.: 'Glass Spherules in the Lunar Dust', *Endeavour* **29**, 135-139.

Before the first Apollo landings on the Moon had taken place, the author had predicted that the lunar surface would be covered with immense numbers of glassy spherules: this prediction was dramatically confirmed when retrieved samples of moon dust were examined. The present article is a report on the author's investigation of dust samples, using a specially developed interferometric technique. Hypotheses are advanced to account for the presence and the abundance of the spherules but further support for such conjectures must await the outcome of future Moon landings.

Warren, N.: 'Elastic Wave-structure Interaction in Granular Material', *EOS* **51**, 347.

Fourteen g of lunar soil were compressed through a series of elastic and inelastic pressure cycles up to about 2 kb. The soil was compressed in a special uniaxial press. Acoustic pulses were applied to the sample by 500 kHz PZT transducers. Compressional velocity, frequency and character of first arrival were observed during the pressure cycles. Velocity and frequency increase in a characteristic fashion as functions of both increasing compaction and pressure. The results may be understood in terms of lattice dynamics and thermodynamic considerations. The lunar soil elastic behavior was found to match that of a lunar microbreccia sample, and leads to a possible interpretation of the seismic behavior of near surface lunar mare regions. (Abstract of a paper presented at the April 1970 meeting of the American Geophysical Union.)

Zeller, E. J., Beard, D. B., and Dreschhoff, G.: 'Weathering Processes and Products on the Lunar Surface', *EOS* **51**, 210.

Two fundamentally different types of weathering processes operate on the lunar surface: those related to the impact of dust grains of micrometeorites, and those caused by radiation effects. The minimum impact velocity of dust grains is 2.38 km/sec, and at this speed the grains and a portion of the target surface will be evaporated. For this reason lunar dust must be considered to be essentially locally derived and not a sample of interplanetary material. Total surface erosion by all grains can be expected to be of the order of one to three meters in 10^9 years. Radiation weathering is much less effective in eroding surfaces than grain impact, but important chemical changes are involved when energetic proton impinge upon silicate rocks. Solar wind sputtering may cause chemical reduction on some surfaces, and solar flare protons can form hydroxyl ions within their range of penetration. The products of the weathering processes are interesting because they provide a possible local source of energy on the Moon. More than 200 cal/g has been measured in proton irradiated olivine and shocked minerals are also known to store energy. The energy is stored in the material in the form of lattice disorder resulting from radiation damage or shock. Release is effected by heating to the point at which the mobility of the displaced atoms is sufficient to permit reordering of the lattice to occur. (Abstract of a paper presented at the March 1970 meeting of the American Geophysical Union.)

12. Photometry of the Moon

Coyne, G. V. and Pellicori, S. F.: 'Wavelength Dependence of Polarization, XX: The Integrated Disk of the Moon', *Astron. J.* **75**, 54-60.

Photoelectric polarimetry of the whole lunar disk in eight wavelength intervals between 0.3 and 0.6 μ at a range of phase angles between 0 and 140 is presented. The observations were made near Tucson and in Hawaii, with a design-study model of a polarimeter for space missions. The polarization is maximum near and 100 phase angle, and it increases progressively with decreasing wavelength. The polarization maximum occurs at smaller phase angles for the longer wavelengths. There is no domain of negative polarization near 180 phase corresponding to the one near 0 phase. For phase angles greater than 40 the electric-vector maximum is perpendicular to the scattering plane and there is no rotation of the plane of polarization within an accuracy of $\pm 2^\circ$. Some excess polarization with the electric-vector maximum in the scattering plane has been found during certain eclipses.

Dollfus, A. and Bowell, E.: 'Polarimetric Properties of the Lunar Surface and Its Interpretation. Part 1: Observations', Air Force Cambridge Research Laboratories-69-0529.

The paper reports on observations and analysis of polarimetric properties of the lunar surface. During the contract two new photoelectric polarimeters were developed, one for infrared and one for ultra-violet light. Part I of the study contains the observational work and is subdivided into two parts. The first part dealt with the polarization characteristics of 14 lunar regions of 65 sec covering the wave-

length range from 0.327 to 1.05 microns. Polarization curves have been obtained for all of these regions. A second set of observations is the determination of the maximum degree of polarization in orange light, of 142 regions, most of which are less than 5 seconds in diameter. The analysis of the measurements of maximum degree of polarization and the normal albedo yields a mathematical interrelation which very probably holds for all lunar terrains. A final portion of this study was the determination of a new lunar normal albedo scale based on measurements provided by nine different sources and the preparation of a catalog of normal albedos of 67 small lunar regions. Part II of the report discusses the application of the polarimetric techniques to the quantitative evaluation of physical properties of small regions on the lunar surface.

Goetz, A. F. H.: 'Apollo-12 Multispectral Photography Experiment', NASA-Contractor's Report-110087; Technical Memorandum-70-2015-1.

The Lunar multispectral photography experiment S-158, was successfully carried out on Apollo-12. A number of photographs were returned in the blue, green, red and infrared portions of the optical spectrum. Preliminary data analysis shows no colour boundaries in the frame containing the Fra Mauro formation and the Apollo 13 landing site. Colour differences were found in the frame containing Lalande η , establishing the existence of small-scale colour differences on the lunar surface.

Goetz, A. F. H., Billingsley, F. C., and Yost, E.: 'Preliminary Results from the Apollo-12 Lunar Multispectral Photography Experiment', *EOS* **51**, 346.

The Lunar Multispectral Photography Experiment was successfully carried out in lunar orbit aboard Apollo-12. Over 100 black and white photographs were returned from four cameras having filters centered in the blue, green, red and photographic infrared portions of the spectrum. Data analysis is carried out by both photographic methods and computer image processing. Color differencing techniques are used on a combination of three filtered photographs. Color calibration is obtained from Earth-based photometry. Preliminary analysis shows no color boundaries in the frame containing the Fra Mauro Formation and the Apollo-13 landing site. Color differences were found in the frame containing Lalande η , establishing the existence of small scale color differences on the lunar surface. (Abstract of a paper presented at the April 1970 meeting of the American Geophysical Union.)

Greenman, N. N. and Gross, H. G.: 'Luminescence Studies of Apollo-11 Lunar Samples', *EOS* **51**, 338.

The luminescence of lunar rocks is being studied to (1) evaluate the reports of lunar luminescence based on astronomical observations, (2) understand how the luminescence behavior reflects the origin and history of the lunar lithologic materials, and (3) discover luminescence characteristics of the rocks that might aid in geologic mapping and other lunar exploration activities. Excitation is with ultraviolet (1216 Å and 2000 to 4000 Å), X-rays, protons, and electrons. Results to date of measurements still in progress show an efficiency with 3000 Å excitation of about 6×10^{-5} for four lunar rocks (one breccia, one coarse-grained igneous, and two fine-grained igneous). This compares with values of about 8×10^{-5} measured for a terrestrial gabbro, very similar in composition to the lunar rocks, and about 10^{-4} for a terrestrial granite. If these are typical values for other ultraviolet excitation wavelengths, the Apollo-11 site appears to contribute little to lunar luminescence; however, higher efficiencies in other areas of the Moon, possibly the highlands, are suggested by an anorthosite component found in the Apollo-11 dust samples. (Abstract of a paper presented at the April 1970 meeting of the American Geophysical Union.)

Gross, H. G. and Greenman, N. N.: 'Luminescence from Middle and Near UV Laser Irradiation of Apollo-11 Lunar Samples', *EOS* **51**, 338.

Chips from lunar rocks (two chips each of breccia, coarse-grained and fine-grained igneous rocks), two terrestrial rocks (granite and gabbro) and one terrestrial mineral (willemite) were irradiated with

UV long wave (3511 and 3638 Å together, around 80 milliwatts) and short wave 2573 Å, around 8 milliwatts) lines from an argon ion laser. Sensing of the spectral scan was by single photon counting from 1050 Å to 6000 Å. Initial results indicate that certain lines are emitted, the wavelengths and intensities of which are dependent on the sample area irradiated. The effective luminescence efficiencies are higher than those reported for other irradiations (electromagnetic and charged particle), in some cases by more than two orders of magnitude. (Abstract of a paper presented at the April 1970 meeting of the American Geophysical Union.)

Hapke, B.: 'Inferences from the Optical Properties of the Moon Concerning the Nature and Evolution of the Lunar Surface', *Radio Sci.* **5**, 293–299.

The unusual optical properties of the Moon are summarized. They imply that the fine-grained, compressible material observed by the Surveyor television cameras is representative of the entire lunar surface and very probably of the surfaces of Mercury, Mars, and the asteroids also. The soil is the result of repeated meteorite impacts and is not an ash flow. Evidence for darkening is examined, and it is concluded that a process is acting on the lunar surface to alter the albedo and color of the rock powder. Materials of chondritic or granitic composition are not prevalent on the Moon. Differences in the optical properties of the maria and the highlands imply that the soil cover is thicker in the highlands than in the maria and that the highland soils are laterally more homogeneous than are those of the maria.

Holt, H. E.: 'Photometry and Polarimetry of the Lunar Regolith as Measured by Surveyor', *Radio Sci.* **5**, 157–170.

Photometric and polarimetric properties of lunar soil and rock fragments were determined from Surveyor pictures. High resolution measurements (centimeter scale) revealed differences in the photometric functions of various materials concomitant with probable different finescale surface textures. The photometric function of the light, undisturbed fine-grained lunar soil is similar to the function measured through an Earth-based telescope (kilometer resolution), whereas the darker, disturbed soil has a more peaked backscatter function, and smooth compressed soil has more Lambertian-like reflectivity. Most rock fragments seem to have essentially dust-free surfaces and a Lambertian-like photometric function; their normal albedos are estimated to range from 9 to 22%. The polarimetric function of lunar soil is similar to that of basalt and gabbro powdered to a grain size of 30 to 75 μ . Lunar rocks reflecting strongly polarized light (up to 34% polarized) have the highest albedos. The observed polarimetric function of lunar rocks is more similar to that of basalt and gabbro than any other common rock type.

Koval, I. K.: *Astrometry and Astrophysics*, No. 1, *Physics of the Moon and Planets*, NASA Technical Translation F-566.

This collection contains the results of photometric investigations of the Moon, Mars and Jupiter. A large amount of the data in this collection concerns the results of a study of the lunar relief, mainly of its far side, by the photometric method; the photographs were obtained by the spacecraft Zond-3.

The results of extensive spectrophotometric observations of Jupiter, carried out in 1964–1966 at the Main Astronomical Observatory of the Academy of Sciences of the Ukrainian S.S.R., are presented, as are calculations of the optical parameters of the Mars atmosphere and surface. The two-channel photometer measuring small light fluxes which was constructed at the Main Astronomical Observatory of the Academy of Sciences of the Ukrainian S.S.R. is described.

This collection is intended for scientific researchers, astrophysicists and geophysicists, as well as for undergraduate and graduate students in the corresponding fields.

Lisina, L. R.: 'A Photometric Method of Lunar Topography', in *Astrometry and Astrophysics*, No. 1: *Physics of the Moon and Planets* (ed. by I. K. Koval – Transl. into English of the Publ.

Astrometriya: Astrofizika, 1, Fizika Lunny: Planet, Kiev, Naukova Dumka Press 1968), NASA-Technical Translation-F-566, 1-33.

The photometric characteristics of the Moon scattering light are described. It is shown that in determining the brightness of lunar details according to theoretical formulae, the macroslope must be considered. Small slopes are determined by the photometric method. The photometric method of determining the slopes for observations of the lunar surface from a spacecraft is discussed. The requisite parameters are calculated in order to determine the slopes and heights of the thalassoid Korolev on the far side of the Moon. From the photographs obtained by the Soviet spacecraft Zond-3, the thalassoid Korolev is a basin surrounded by numerous rings with faults.

McCord, T. B. and Westphal, J. A.: 'Spectral Reflectivity of the Lunar Surface', *EOS* **51**, 338.

An observational study of the spectral reflectance (0.30 to 2.50 microns) of various areas of the lunar surface was carried out. The 60-inch telescope at the Cerro Tololo Interamerican Observatory, Chile, and the 24 and 60-inch telescopes on Mount Wilson, California were used. Both the *ratio* of reflectivities between lunar areas and the normalized *spectral reflectivities* of various lunar areas were determined. The results are: (1) for the first time a narrow 0.95 micron absorption band (not a broad 1 micron band as has been reported by others) has been positively identified in the lunar spectrum; (2) this 0.95 micron band varies in strength and shape with lunar area; (3) there is no well defined absorption band present except for the 0.95 micron band; (4) from the data available, there is a correlation between increasing strength of the 0.95 micron band and decreasing overall slope of the reflectivity curve; (5) a comparison of our Earth-based data for Tranquillity Base with measurements of Apollo-11 soil samples by John Adams shows excellent agreement; (6) both the 0.95 micron band and the overall shape of the curve contain mineralogical information which, with ground-truth, can be extended over the lunar surface. (Abstract of a paper presented at the April 1970 meeting of the American Geophysical Union.)

Mills, A. A.: 'Transient Lunar Phenomena and Electrostatic Glow Discharges', *Nature* **225**, 929-330.

The author proposes that the obscuration associated with transient lunar phenomena is due to fine dust raised by lunar degassing. In certain areas, sporadic escape of accumulated gas occurs through channels opened by tidal stress. Movement and separation of the heterogeneous particles result in separation of charge and, occasionally, sufficient potential difference is built up to promote glow discharge through the transient gas phase. The predominance of hydrogen in the discharge gives the reddish tint.

Minnaert, M. G. J.: 'The Effect of Pulverization on the Albedo of Lunar Rocks', *Icarus* **11**, 332-337.

Measures of the albedo under full-moon conditions have been made on two samples of very dark rocks, pulverized and sieved so as to obtain powders of different grain size. Below a size of 0.05 mm the albedo suddenly increases, obviously because the individual grains become transparent. By a rough calculation of the radiation transfer this is made understandable and a relation is found between the grain size and the absorption coefficient necessary to produce in combination an albedo of 0.10. If the Moon is covered by fine dust, its low albedo shows that the absorption coefficient must be very high, probably because of darkening by the solar wind.

Minnaert, M. G. J.: 'Retro-reflexion', *Nature* **225**, 718.

The article by J. A. Howard, 'Increased Luminance in the Direction of Retro-reflexion - A Recently Observed Natural Phenomenon', is identical with the heiligenschein, extensively discussed in the classical book of Pernter-Exner, *Meteorologische Optik*. It is the opposition effect, which has been studied many times on objects of planetary astrophysics: Saturn's rings, the zodiacal light, the plane-toids and the Moon.

O'Leary, B. T. and Briggs, F.: 'Optical Properites of the Apollo-11 Lunar Samples', *EOS* **51**, 338.

Lunar powder samples returned by Apollo-11 are remarkably similar in their optical properties to those measured for a several km² area surrounding Tranquillity Base, suggesting a ubiquitous covering of the same material in the region. However, there are minor exceptions to the close match: the powder sample shows larger polarizations and a larger opposition effect than would be expected from previous observations. In the spectrum of the lunar rock samples, we detected a strong, broad absorption near 1 μ and a weaker band \gtrsim 1.8 μ which may be due to orthopyroxenes in the presence of other iron-bearing silicates. The 1- μ band was absent in the powder sample (presumably because the particle sizes were too small), which suggests that the spectrophotometer may become a valuable tool in distinguishing between rocky and dusty areas on the Moon. (Abstract of a paper presented at the April 1970 meeting of the American Geophysical Union.)

Pikkarainen, T.: 'The Surface Structures of the Moon and Mercury Derived from Integrated Photometry', *Ann. Acad. Scientiarum Fennicae*, Series A, 6. Physica, 316.

The integrated brightnesses of the Moon and Mercury are theoretically calculated by using a surface model with parabolical holes, Lommel-Seeliger's reflection law and the phase function of the irradiated basalt powder. The theoretical integrated brightnesses are fitted with observations by using two free parameters which describe the surface structures of the Moon and Mercury. The results show that Mercury's surface is more densely covered with holes but that their depths are smaller than on the Moon.

Shevchenko, V. V.: 'A Physical Mapping of the Moon from Photometric Data', *Astron. Zh.* **47**, 599-609.

Problems of the compiling and interpretation of photometric maps of the lunar surface are stated. A material, obtained with AIM 'Zond-2' for the part of the reverse side of the Moon, is used. On the basis of B. Hapke's 'improved' formula systems of equation for 403 parts of the surface are compiled. Parameters ρ_0 , h , γ of Hapke's formula are unknown in the mentioned equation. As the results of the solution of the system of equations maps of the distribution of the surface - the apportionment of districts by types of a photometric relief - is carried out. With average values $\rho_0 = 12.4$, $h = 1.0$, $\gamma = 75^\circ$ (for the value $f = 0.75$), variations of values of these parameters, conditioning the exposing of 6 types of the photometric relief, are observed.

The individual division into districts leads to the conclusion that with the average porosity of the cover matter about 70%, determined from the value h , separate parts are characteristic by increase or decrease of it. From the value in common, with values h , regions, apparently, differing by clusters of stones, are picked out.

Younkin, R. L.: 'Optical Reflectance of Local Areas of the Moon', *Astron. J.* **75**, 831-841.

Photoelectric measurements of the solar energy from 0.31 to 1.1 μ reflected from the lunar crater Plato have been made at the Mount Wilson Observatory. The surface radiance, in absolute energy units, and the radiance factor have been determined for 50-Å bands. Several possible absorption and luminescent features of undetermined origin were found in the visible reflection spectrum. The upper limit to their amplitudes is six per cent. Absorption due to ferrous iron is present, ferric iron is not. The measured radiances and radiance factors, determined for given phase angles, have been combined with photometric functions and colour-phase variations to obtain their values at other phase angles. The V magnitude radiance factor of Plato at zero phase angle was found to be 0.14. This value contradicts the hypothesis of Gehrels, Coffeen, and Owings that there exists a temporal variation of lunar brightness related to the solar cycle. Plato exhibits reddening with phase to the long-wavelength limit of the measurements. The Plato measurements were combined with the ratio measurements of McCord and of McCord and Johnson to obtain relative radiance factors for 86 lunar areas. The visible spectral region has been characterized by the ratio of the reflectance at 0.70 μ to the reflectance at 0.40 μ . The value of this parameter varies only from 1.10 to 1.51, with most areas in the very restricted range from 1.3 to 1.4. Comparison with reflectance of laboratory rock samples and the elemental composition and particle size as determined by the Surveyors indicates the lunar surface material is best approxi-

mated by a Little Lake type basalt with a substantially larger portion of opaque particles. All the lunar areas exhibit a broad shallow absorption centered near 1.0μ and attributed to ferrous iron. In general, the maria have more iron than the uplands, in agreement with the limited findings of the Surveyors. The maria exhibit a trend: the redder the mare, the more the iron; the uplands do not. Plato was found to be an area with a relatively large amount of iron consistent with measurements of infrared emissivity of lunar areas.

13. Thermal Emission of the Lunar Surface

Bastin, J. A. and Gough, D. O.: 'Intermediate Scale Lunar Roughness', *Icarus* **11**, 289–319.

A model surface consisting of parallel troughs has been examined in order to assess the importance of roughness in accounting for the properties of lunar thermal radiation. Insolation, emission from the surface, reabsorption of emitted radiation, and conduction are all considered. Brightness temperatures both in the midinfrared and microwave region are computed for eclipse and lunation conditions, not only as a function of lunar phase, latitude, longitude, and direction of observation, but also for a variety of trough dimensions.

All those features of the observed thermal radiation which cannot be accounted for on the basis of a plane homogeneous model are listed and the extent to which they can be accounted for by the proposed model is considered. In particular, a model for which the width and height of the raised portions are both equal to a quarter of the trough interval gives good agreement with the directional effects observed for lunar daytime radiation in the 10–14 μ wavelength band. In addition a number of other anomalies, including some already accounted for in the literature by other causes, receive more or less good explanations on the basis of roughness.

Clegg, P. E. and Carter, B. S.: 'Measurements of Lunar Radiation in the Wavelength Range Centred at 1.2 mm', *Monthly Notices Roy. Astron. Soc.* **148**, 261–274.

The results of several investigations of the lunar surface thermal properties are reported including observational and theoretical considerations of the effect of roughness on the polarization of this radiation. It is concluded that roughness plays an important part in determining the millimetre wavelength thermal emission of the Moon. In particular the difference in temperature between Moon and highlands and the observed poleward darkening function may be attributed to roughness.

An effective dielectric constant for the surface material is deduced and a tentative model for the centimetre scale roughness of the surface advanced. It appears that roughness increases as the scale on which it is observed decreases.

Langseth, M. G., Jr., Wechsler, A. E., Drake, E. M., Simmons, G., Clark, S. P., Jr., and Chute, J., Jr. 'Apollo-13 Lunar Heat Flow Experiment', *Science* **168**, 211–217.

The article describes an experiment to make the first direct measurement of the lunar surface heat flow which is supposed to be emplaced on the Moon during the Apollo 13 mission. The measurement consists of making independent determinations of the vertical temperature gradient in the lunar surface, as a function of time, and of the thermal conductivity of the surrounding lunar soil. These data will provide a year-long history of the heat flux through the upper 3 meters of the lunar subsurface. The balance of this heat budget will represent the steady-state loss of heat from the interior of the Moon at the Apollo-13 site, Fra Mauro. The value of heat flow measured by this experiment will set constraints on the interior temperature and composition of the Moon.

Logan, L. M. and Hunt, G. R.: 'Effect of a Vacuum on the Emission Spectra of Particulate Rocks and Minerals', *EOS* **51**, 337.

Diagnostic compositional information is contained in the infrared emission spectra of rocks and minerals. In some remote sensing situations, such as when data is acquired from the Moon, the surface materials are under a hard vacuum and are heated by the Sun. To simulate such a situation we have

applied a hard vacuum to particulate rock and mineral samples, and have varied both the particle size and means of heating. We find that these variables cause dramatic changes in both the intensity and position of the principal Christiansen frequencies, and in the overall appearance of the spectra. The magnitude of these effects and an explanation for them will be discussed. (Abstract of a paper presented at the April 1970 meeting of the American Geophysical Union.)

Mendell, W. W. and Low, F. J.: 'Low-Resolution Differential Drift Scans of the Moon at 22 Microns', *J. Geophys. Res.* **75**, 3319-3324.

Differential drift scans were made across the 3-day-old Moon at a wavelength of 22 μ with a beam-width of 2'.4. Measured cold limb brightness temperatures ranged from 102K in the equatorial region to 84K in the southern polar regions. Certain scans were processed to reveal the temperature distribution from the cold limb to the sunrise terminator. The portion of the lunar 'cooling curve' that was obtained by this method agrees well with the portion measured by previous investigators who made infrared scans from the sunset terminator into unilluminated regions.

Murcray, F. H., Murcray, D. G., and Williams, W. J.: 'Infrared Emissivity of Lunar Surface Features: 1. Balloon-borne Observations', *J. Geophys. Res.* **75**, 2662-2669.

The thermal emission spectra (7.0 to 13.5 μ) of six selected areas on the lunar surface were measured from an altitude of 32 km and their spectral emissivities calculated. All spectra show departures from black- or gray-body emission. Emissivities in the 8.0- to 9.0- μ region of the spectrum are significantly higher than those for wavelengths greater than 10 μ . Differences are noted in the wavelengths of peak emissivity, particularly between the highland areas and the maria. The interpretation of the differences in terms of lunar composition is discussed in Part 2.

Salisbury, J. W.: 'Composition of the Moon from Balloon-borne Mid-infrared Observations', *Radio Sci.* **5**, 241-246.

Mid-infrared spectra (7.0 to 13.5 μ) of six different areas on the lunar surface have been obtained from an altitude of 31 km by using a 24-inch balloon borne telescope. All spectra show significant departures from blackbody or graybody emission, in particular displaying a peak in emissivity that varies in wavelength from 8.11 to 8.37 μ . The position of this peak varies regularly with type of surface feature in the field of view. Laboratory studies show that the wavelength of peak emissivity in surface emission can be interpreted in terms of rock composition, and that the differences in peak emissivity from place to place result from differences in rock type. Barring some unanticipated systematic error, the data obtained so far indicate that the two circular maria, Imbrium and Serenitatis, are ultrabasic in composition, whereas the lunar crust appears to be basic in composition. This compositional heterogeneity may explain the location of major mascons in the circular maria.

Salisbury, J. W., Vincent, R. K., Logan, L. M., and Hunt, G. R., 'Infrared Emissivity of Lunar Surface Features: 2. Interpretation', *J. Geophys. Res.* **75**, 2671-2682.

Thermal emission spectra of six different areas on the lunar surface are discussed in the light of laboratory studies of the spectral emissivity of rocks and minerals. It is shown that the emission maxima characteristics of lunar spectra are similar to emission maxima found in the spectra of particulate rock samples. Such emission maxima are shown to be diagnostic of general rock type, within limits that are defined. Differences in emission maxima of their respective spectra indicate a significant difference in bulk composition between the material ejected by the craters Copernicus and Theophilus and the surface material of the two circular maria, Imbrium and Serenitatis. Barring some unknown measurement error in the spectra, or some unanticipated effect of the lunar environment on surface spectral behavior, we can conclude that the crater materials display an emissivity maximum characteristic of silica-poor basic rocks, while the circular maria display a maximum characteristic of silica-rich ultrabasic rocks. If this preliminary result is confirmed by future research, it has profound implications for the origin and evolution of the lunar crust.

Shchuko, O. B.: 'Inhomogeneous Properties of Lunite in the Subsurface Layer', *Soviet Phys. – Astron.* **13**, 989–992.

An inhomogeneous model of the lunar surface layer is formulated on the assumption that the thermal parameters (heat conductivity and heat capacity) are dependent on temperature. It is shown that the surface temperatures at lunar midnight and in the middle of an eclipse, computed for the examined model, agree well with the surface temperatures indicated by radio measurements at infrared wavelengths; surface matter density in the lunar surface layer increases by not more than 10% at a depth of 3–4 cm and then remains constant to a depth of 3–4 m.

Starodubtsev, A. M.: 'Long-term Measurements of Lunar Radio Emission at 3.2 cm', *Soviet Astron. – AJ* **13**, 514–516.

Measurements of lunar radio emission performed at 3.2-cm wavelength by the artificial-moon method from 1964 to 1966 yield a value of 213.6 ± 0.24 K for the constant component of the Moon's effective temperature, averaged over the disk. The amplitude of the first harmonic of the lunation frequency was 10.2 ± 0.37 K, and the phase lag in the maximum of the radio emission relative to full-moon was $44^\circ \pm 3^\circ.5$.

Winter, D. F.: 'The Infrared Moon: Data, Interpretations, and Implications', *Radio Sci.* **5**, 229–240.

Measurements of infrared radiation from the Moon are used to estimate the thermophysical properties of the lunar soil and to infer the general nature of small-scale surface relief. Directional emission characteristics of the illuminated surface are probably associated with small craters of recent origin. On the other hand, abnormal populations of exposed rocks are thought to be responsible for many of the localized thermal enhancements observed during an eclipse. Implications of infrared measurements regarding the evolution of the surface are described.

14. Electromagnetic Properties of the Moon

Chatelain, A., Kolopus, J. L., and Weeks, R. A.: 'Radiation Effects and Oxygen Vacancies in Silicates', *Sci.* **168**, 570–571.

Proton and electron irradiation of silicates, minerals, and rocks produces a paramagnetic defect whose resonance spectrum is identical to that of the singly charged oxygen vacancy in silica glass and α -quartz. It is suggested that this defect is characteristic of all structures containing SiO_4 tetrahedra. Cracks, fracturing, and electric discharges have been observed after irradiation in planes determined by the particle ranges. These processes may contribute to the erosion and transport of lunar surface materials.

Dey, A., Morrison, H. F., and Ward, S. H.: 'Electric Fields from a Horizontal Electric Dipole Situated above a Layered Lunar Half-space', NASA-Contractor's Report-73 456.

Dyal, P., Parkin, C. W., and Sonett, C. P.: 'Apollo 12 Magnetometer – Measurement of a Steady Magnetic Field on the Surface of the Moon', *Science* **169**, 762–764.

The Apollo-12 magnetometer has measured a steady magnetic field of 36 ± 5 gammas on the lunar surface. Surface gradient measurements and data from a lunar orbiting satellite indicate that this steady field is localized rather than global in its extent. These data suggest that the source is a large, magnetized body which acquired a field during an epoch in which the inducing field was much stronger than any that presently exists at the Moon.

Fuller, B. D. and Ward, S. H.: 'Theoretical Calculation of the Electromagnetic Response of a Radially Layered Model Moon', NASA-Contractor's Report-73436.

To inquire how layering would affect the concept of the electromagnetic behavior of the lunar sphere and to what extent the possibility of layering should be considered in the design of an experiment to determine the electrical properties of the lunar interior a model is used of a multi-layered sphere excited by a plane electromagnetic field. The layers are concentric and each layer is assumed to have constant electrical parameters chosen according to best estimates.

Helsley, C. E.: 'Evidence for an Ancient Lunar Magnetic Field', *EOS* 51, 348.

Magnetic studies on the samples returned from the Apollo 11 and 12 missions have shown that many of the rocks contain stable magnetic moments. The primary carrier of the magnetization is native iron or iron-nickel alloys. Troilite is also present and gives a magnetic Mossbauer spectrum. Progressive thermal demagnetization experiments on some of the samples suggest that the magnetization of these rocks was acquired on the Moon in the presence of an applied field in the range of 1000 to 2000 gammas provided that the magnetization was acquired as a result of cooling through the Curie point. This implies that either the Moon had a weak magnetic field 3.5 to 4.0 aeons ago, and thus a small conducting fluid core, or that it was in the immediate vicinity of another body that had a magnetic field, e.g. the Earth. (Abstract of a paper presented at the April 1970 meeting of the American Geophysical Union.)

Hills, H. K., Freeman, J. W., Jr., and Balsiger, H.: 'Energetic Protons Observed at the Lunar Surface on the Night Side of the Moon', *EOS* 51, 407.

The Rice University lunar ionosphere detector carried to the lunar surface by the Apollo-12 astronauts has recorded fluxes of energetic protons during the lunar night. These fluxes fall into two categories of energy spectra. The first consists of protons in the 1 to 3 keV energy range. These ions are seen sporadically early in the lunar night. They are thought to be energetic protons escaping upstream from the bow shock. The second category of spectra is that exhibiting solar wind energy ions. These ions are found as far as 45° around from the terminator on the night side. (Abstract of a paper presented at the April 1970 meeting of the American Geophysical Union.)

Ness, N. F.: 'Interaction of the Solar Wind with the Moon', NASA-Technical Memorandum-X-63 888.

The current state of experimental and theoretical studies of the interaction of the solar wind with the Moon is reviewed. The Explorer-35 has provided since July 1967 definitive experimental results regarding the perturbations of the interplanetary magnetic field and plasma in the lunar wake. The Moon appears to behave as a nonmagnetic, nonelectrically conducting fully absorbing spherical obstacle in the solar wind flow. The principle features of the plasma field perturbations are the following: A downwind plasma umbral void containing an enhanced interplanetary magnetic field only slightly perturbed in direction. A downwind penumbral region aft of a rarefaction wave or Mach cone, elliptical in cross sectional geometry, contains a reduced plasma flux and magnetic field. A very limited penumbral region, upwind of the lunar Mach cone, sometimes contains an enhanced magnetic field and plasma flux. A broad region both upstream and downstream from the lunar wake is connected to it by the interplanetary magnetic field in which rapid fluctuations of the magnetic field occur with an amplitude that decreases with distance from the wake.

Snyder, C. W., Clay, D. R., and Neugebauer, M.: 'Initial Results from the ALSEP Solar Wind Spectrometer', *EOS* 51, 407.

The ALSEP solar wind spectrometer was set up on the lunar surface by the Apollo-12 astronauts and has been operating continuously since 15.25 UT, November 20, 1969. Full-sky coverage and energy (per unit charge) analyses of both positive ions and electrons is obtained by an array of 7 modulated Faraday cup detectors. The detection threshold is 3×10^6 normally-incident, singly-charged ions/cm²

sec/energy window ($\Delta E/E = 0.34$ for protons, 0.67 for electrons). data In the first month of operation, the data showed, at the appropriate times, (1) fairly typical solar wind positive-ion fluxes arriving from close to the solar direction, (2) magnetosheath positive-ion fluxes similar to those measured on other spacecraft, or (3) no measurable flux, both in the geomagnetic tail and during the lunar night. The data, especially near sunrise and sunset, are being compared with solar plasma measurements on Earth satellites to determine whether any alteration of the plasma by the Moon is detectable. (Abstract of a paper presented at the April 1970 meeting of the American Geophysical Union.)

Ward, S. H.: 'Scientific Rationale For Apollo Lunar (Orbital) Electromagnetic Sounder Experiment; Final Technical Report', NASA Contractor's Report 73435.

A Lunar Electromagnetic Sounder experiment is tentatively scheduled to be part of the science payload in the mission of Apollo-19. In basic concept, the experiment requires transmission of electromagnetic waves from the spacecraft in orbit, reflection of these waves from the Moon, and subsequent reception of the waves at the spacecraft. The complex ratio of received signal to transmitted signal provides information which may be interpreted in terms of the threedimensional distributions of electrical conductivity, dielectric constant, and magnetic permeability in the lunar interior.

Ward, Stanley H.: 'Electromagnetic Exploration of the Moon', NASA Contactor's Report-73378.

Whang, Y. C.: 'Two-Dimensional Guiding-Center Model of the Solar Wind-Moon Interaction', NASA-Technical Memorandum-X-63845; X-682-70-61.

This paper presents a continued study of the two-dimensional guiding-center model of the solar wind interaction with the Moon. The characteristics theory and the computational method are discussed. The magnetic permeability of plasma is $1/(1 + \beta/2)$ in the solar wind flow upstream of the Moon, and it changes to 1 in the void region of the lunar wake. The gradual change of the magnetic permeability in the penumbral region from the interplanetary condition to the void condition is explained as the source of field perturbations in the lunar wake. Perturbations of the magnetic field propagate as magnetoacoustic waves in a frame of reference moving with the plasma flow. Computer solutions were obtained to show that (1) the two principal perturbations of the magnetic field in the lunar wake (the umbral increase and the penumbral decrease) are confined to a region bounded by a Mach cone tangent to the lunar body, and (2) the penumbral increases occur outside the lunar Mach cone. Computer solutions are also used to identify the source of field perturbations and to simulate the solar wind-Moon interaction under varying interplanetary conditions.

15. Exploration of the Moon by Spacecraft

Allenby, R. J.: 'Lunar Orbital Science', *Space Sci. Rev.* **11**, 5-53.

Orbital science has, to the present, concentrated on studies of force fields, particles, and visible photography. Cameras have been the major scientific instrument (it could be debated that for geodesy and gravity the entire spacecraft represents an instrument), and geology has been the principle benefactor. Photography has also been essential for the manned landing program, which would not have been possible on the schedule followed without the detailed Lunar Orbiter pictures.

Orbital tracking data indicates that the Moon is almost homogeneous with perhaps a slight increase in density with depth. Significant analysis of the higher gravity harmonics have identified localized, near surface gravity highs that appear to be associated with circular maria. The Moon does not have a significant magnetic field of its own, and the solar wind appears to impinge directly on the surface. Russian and United States evidence on micrometeorite fluxes near the Moon is conflicting, but probably there is a decrease in flux compared to that near the Earth.

Photographic evidence indicates that both impact and volcanic action has shaped the lunar surface. Mass movements of surface material and surface erosional effects are clearly evident. Surface water

in the past, or near surface permafrost now, are definite possibilities to explain the sinuous rills. Faulting, both regional and local, is evident, as is probably horizontal layering near the surface.

The United States space program is embarking on a broad program of orbital science including nearly the entire spectra of remote sensing. Approved orbital missions extend through 1972 and will be carried out in conjunction with manned landings. Emphasis will be placed on determining the extent and degree of surface variations between and within lunar provinces and the nature and strength of the lunar spectrum. Information obtained from the surface missions and the returned lunar samples will be invaluable in helping us to design orbital instruments and interpret the results.

Missions after 1972 undoubtedly will carry more instruments that will give us definitive information on the geochemical nature of the lunar surface and interior.

Arnett, G. M.: 'Lunar Excursion Module RCS Engine Vacuum Chamber Contamination Study', NASA-Technical Memorandum-X-53859.

The objective of this study was the definition of future contamination studies and procedures, and the investigation extended to the effects of the Reaction Control System (RCS) plume on optical flight experiments. This report is concerned with the effects of the RCS plume deposits on the test beds along with the characteristic changes that occur once these deposits are exposed to the laboratory atmosphere. Test beds consisting of various optical surfaces were exposed to an LM-RCS rocket engine plume in the vacuum chamber. Analysis of the contaminated test beds included optical measurements ranging from the near-ultraviolet through the far-infrared region together with mass spectrometer identification of the deposits. This study demonstrates that the instrumental procedures and sample handling are insufficient in many ways; however, the experience gained has led to an improvement of laboratory techniques and has greatly facilitated the interpretation of the results. In some cases, more suitable apparatus has been utilized that will enhance data analysis from planned orbital flight contamination experiments.

Benschoter, C. A., Allison, T. C., Boyd, J. F., Brooks, M. A., Campbells, J. W., Groves, R. O., Heimpel, A. M., Mills, H. F., Ray, S. M., Warren, J. W., Wolf, K. E., Wood, E. M., Wrenn, R. T., and Zein-Eldin, Z.: 'Apollo 11: Exposure of Lower Animals to Lunar Material', *Science* **169**, 470-472.

Lunar material returned from the first manned landing on the Moon was assayed for the presence of replicating agents possibly harmful to life on Earth. Ten species of lower animals were exposed to lunar material for 28 days. No pathological effects attributable to contact with lunar material were detected.

Binder, A. B. and Roberts, D. L.: 'Criteria for Lunar Site Selection', NASA-Contractor's Report-110199; p-30.

The basic framework for lunar exploration is that Apollo missions will visit sites that are representative of the major provinces of the Moon and will have as a principal function, the collection of samples from the regions visited. A brief critique of the selected Apollo sites is included and within the context state above, seven of the ten sites conform extremely well. The criticism of the other three, site 5 (recycle), Rima Bode II, and Descartes is that they are too complex to allow unambiguous interpretation of the collected samples. The principle task is to understand the individual processes that have operated on the Moon over its lifetime. Type sites containing features that are unambiguously representative of individual processes are listed. The requirements for adequate exploration of each type site (such as the daytime, number of mean and lunar science specialists require, and the extent of mobility) are defined.

Boeing Co., Houston, Tex. Electrical/Electronics Technology: 'Modifications to the Lunar Orbiter Ground Reconstruction Equipment', NASA-Contractor's Report-108376.

Bureau of Mines, Minneapolis, Minn. Twin Cities Mining Research Center: 'Multidisciplinary Research Leading to Utilization of Extraterrestrial Resources', NASA Contractor's Report-109399.

Chang, G. K., Gunther, P., and James, D. B.: 'A Secondary Ejecta Explanation of a Lunar Seismogram', NASA-Contractor's Report-110079; Technical Memorandum-70-2015-2.

The seismograph recording of the Apollo-12 Lunar Module impact is studied as the result of a spray of secondary ejecta around the seismometer. A theoretical study of the ballistic trajectories, plausible angular distributions and seismic signals to be expected from such a spray was made. Secondary ejecta cannot account for signals arriving earlier than 45 sec, but could explain the remaining portion of the signal provided that the angular distribution of the secondary ejecta are assumed to peak sharply in the vertical direction. Hence, it is concluded that one can neither prove nor disprove the hypothesis that a substantial portion of the signal is due to secondary ejecta.

Coryell, R. B. and Durr, L.: 'Crater Deflection Studies', NASA-Contractor's Report-109460.

The purpose of the experiments reported in this document was to gain a first-order understanding of the deflection of which a vehicle, with wheels locked in a dead-ahead position as it traversed a crater, would be subjected. These experiments involved a statistical test using a model vehicle that traversed craters constructed in sand. No attempt was made either to scale the vehicle to experimental size or to simulate the lunar environment. Rather, the objective was an inexpensive, large statistical sample of the crater deflection of a model vehicle. Results from these stochastic experiments provide hints as to some properties of such a model and data for calculation of some limited performance characteristics of a wheeled vehicle on the cratered surface of the Moon. This document reports the experimental apparatus and procedures, a statistical summary of the experimental data, and salient features of the results.

Cox, K. J.: 'A Case Study of the Apollo Lunar Module Digital Autopilot', NASA-Technical Memorandum-X-58044.

Dickerman, P. J.: 'The Role of Sub-satellites in the Exploration of the Moon', NASA-Contractor's Report-110186; P-33.

The need for Apollo CSM sub-satellite orbiters as a subset of a broader class of lunar orbiters is considered. The basis of the evaluation is the orbital science measurements which should be performed in the exploration of the Moon. Consideration is given to all modes of investigation except photography. A sub-satellite is defined as a spacecraft which initially is incorporated in the service module, which is released in or into lunar orbit, and which can function completely independent of the service module. Its complexity may range from a simple beacon to a large automated spacecraft and the relevance of subsatellites over this whole range is considered.

Elefant, J., Lavan, E., and Veshlage, E.: 'Hazard Detection Methods for a Lunar Roving Vehicle', NASA-Contractor's Report-102510.

A system is investigated which is capable of detecting potential hazards to a lunar roving vehicle and preventing it from moving into a position which would disrupt the mission. Sensors or combinations of sensors were studied for radio frequency wave propagation above or through the lunar surface and seismic wave propagation through the lunar surface. Pulse and FM-CW radars were considered for a surface detection system and seismic techniques and soil penetrating radar were considered for a subsurface detection system. The physical performance impact on LRV capability were determined from the sensor investigations.

Freitag, D. R., Green, A. J., and Melzer, K. J.: 'Performance Evaluation of Wheels for Lunar Vehicles', NASA-Contractor's Report-110252.

One pneumatic and four metal-elastic wheels were laboratory tested in a fine sand to determine their relative performance and to establish a better understanding of the basic principles of the interaction of lightly loaded wheels with soil that is basically frictional, but with a small amount of cohesion. Five levels of sand strength, representing cohesion values ranging from 0 to 0.26 psi were used. The cohe-

sional and frictional properties spanned a range that is believed to include the probable range of lunar soil properties. Programmed slip tests, in which the slip of the wheel was varied from negative to high positive values, were conducted with a single-wheel dynamometer system. The average speed of the system at zero slip was approximately 0.5 m/sec. Wheel loads were varied from 67 to 670 N to ascertain the effect of load on performance. Data indicate that for loads less than about 220 N, the pull coefficient was constant for a given soil condition. At greater speeds, the rate of increase in the performance coefficient decreased.

Hartmann, W. K. and Sullivan, R. J.: 'Objectives of Permanent Lunar Bases', NASA-Contractor's Report-110187; p-32.

Hartmann, W. K.: 'Lunar Surface Scientific Experiments and Emplaced Station Science', NASA-Contractor's Report-110200; p-31.

The relation of science stations (of the ALSEP type) to the total conglomerate of lunar science is summarized. A comprehensive list of scientific objectives and measurement techniques from which to draw the experiments and fit them to the various landing sites is determined. The different phases of lunar exploration and the specific type-sites and experiments to be considered for each are discussed. Emphasis is on Apollo and the immediate post-Apollo period, though orbital and permanent surface base operations are considered. The experiments, the sites, and the rationale of lunar research are established and the surface science experiments are selected and ranked according to importance for Apollo and for post-Apollo missions. The possible needs for remote unmanned landers, unmanned and manned rovers, and flying units are considered. Manned rovers and flying units are found most useful.

Hedden, R. O.: 'Study of the Thermal Conductivity Requirements. Volume 2: Multiple Docking Adapter Thermal Model', NASA-Contractor's Report-102603.

Two mathematical models, for use in detailed thermal analyses of the multiple docking adapter, were developed and checked out. These were: the multiple docking adapter thermal model and the Apollo Applications Program cluster thermal model which determine the steady-state and/or the transient temperature distribution throughout the multiple docking adapter for a completely realistic set of boundary conditions. These models were written for use with two existing computer programs: The heat rate computer program, and the Mark 5C thermal analyzer. These two programs provide the capability for complete thermal analyses of the multiple docking adapter in any of its many planned orbital configurations. The effect of module rearrangements, surface finish changes, solar panel and module configuration changes can be evaluated. Also, internal heat load changes, experiment surface finish changes, structural changes, as well as most of the other changes which affect the multiple docking adapter temperature distributions can be evaluated using these computer models.

Heydegger, H. R. and Turkevich, A.: 'Radioactivity Induced in Apollo-11 Lunar Surface Material by Solar Flare Protons', *Science* **168**, 575-576.

Comparison of values of the specific radioactivities reported for lunar surface material from the Apollo-11 mission with analogous data for stone meteorites suggests that energetic particles from the solar flare of 12 April 1969 may have produced most of the cobalt-56 observed.

Hill, P. R. and Thomas, D. F., Jr.: 'Kinesthetic Control Simulator', NASA-Case-Langley Research Center-10276-1.

A control simulator for permitting an operator to obtain experience in multiple degree freedom of movement of a vehicle similar to a lunar flying platform is described. The kinesthetic control simulator has a flat base upon which rests a support structure having a lower spherical surface for rotation on the base plate with columns which support a platform above the support structure at a desired location with respect to the center-of-curvature of the spherical surface. A handrail is located at

approximately the elevation of the hips of the operator above the platform with a tilt ring attached to the support structure which may be used to limit the angle of tilt. Five degree freedom of rotation can be obtained by utilizing an air pad structure or dolly for support of the control simulator.

Hillenbrand, R.: 'The Apollo-12 Explorers on the Moon', *Sky Telesc.* **39**, 95-98.

The surface explorations are described and several photographs of the lunar surface are presented.

ILT Research Institute: 'Logic for Lunar Science Objectives', NASA-Contractor's Report-110179; p-29.

James, D. B., Chang, G. K., and Gunther, P.: 'Secondary Ejecta Explanation of a Lunar Seismogram', *EOS* **51**, 347.

It has been suggested that the seismograph recording of the Apollo-12 Lunar Module impact was the result of a spray of lunar dust around the seismometer rather than the result of seismic waves propagated through the Moon. We have made a theoretical study of the ballistics trajectories, plausible angular distributions and seismic signals to be expected from such a spray. It is concluded that dust particles could produce a signal similar to the observed one and that some part of the observed signal may be due to the secondary debris falling close to the seismometer. If the signal is primarily due to secondary particles then it is predicted that the impact of the SIVB at a different range will give rise to a signal onset corresponding to a flight velocity of 1.7 km/sec as compared to the 3-4 km/sec measured by Latham and that if the Apollo-13 Lunar Module is impacted between the Apollo 12 and 13 seismometer as is currently planned, that the Apollo-12 seismometer will have a larger signal due to anisotropies in the angular distribution of the secondary particles.

Jet Propulsion Lab., Calif. Inst. of Tech., Pasadena: 'Future Projects', Jet Propulsion Lab., *Space Programs Sum.* **3**, 37-60.

Karafiath, L. L. and Mohr, G.: 'The Effect of Ultrahigh Vacuum on the Friction Between Various Solids and Granular Soils', Grumman Aircraft Engineering Corp.-RE-376.

The initial and kinetic friction developing in ultrahigh vacuum between various solids and ground basalt was measured in an apparatus designed for this purpose. The solid materials used in the ultrahigh vacuum tests were titanium and fiberglass; the particle size range of the ground basalt was 250-500 μ . The results of these and the earlier experiments with steel showed that the total frictional resistance between the various solids and soils tested invariably increases in ultrahigh vacuum but in a different way for the various combinations of materials. The kinetic friction for steel on basalt increased by a constant adhesion, while for both titanium and fiberglass the coefficient of kinetic friction increased appreciably while the adhesion decreased slightly. The increase in the initial friction was significant for fiberglass and steel and negligible for titanium. The use of the experimental relationships between normal stress and frictional resistance for the computation of traction that wheels can exert is discussed.

Kollsman Instrument Corp., Syosset, N.Y., General Motors Corp., Milwaukee, Wis.: 'Apollo Optical Subsystem and LM Alignment Optical Telescope, Volume 2, Report', NASA Contractor's Report-108359.

Kollsman Instrument Corp., Syosset, N.Y., General Motors Corp., Milwaukee, Wis.: 'Apollo Optical Subsystem and LM Alignment Optical Telescope; Volume 2, Part 2; Final Report', NASA Contractor's Report 108360.

The functions of an Apollo Reliability group concerned with the manufacture of optical equipment

for the Apollo spacecraft and Lunar Module are described. The group assured the reliability of the product by establishing standards of workmanship, techniques of manufacture, techniques and standards for measurement of achieved reliability, and by indoctrinating personnel with reliability concepts and reliability consciousness. A reliability program was established to determine reliability requirements through reliability analyses, environmental analyses, design review, test planning, and selection of parts and materials for the Apollo optical subsystem.

Latham, G. V., Ewing, M., Press, F., Sutton, G., Dorman, J., Nakamura, Y., Toksoz, N., Wiggins, R., Derr, J., and Duennebier, F.: 'Passive Seismic Experiment', *Science* **167**, 455-457.

Seismometer operation for 21 days at Tranquillity Base revealed, among strong signals produced by Apollo-11 lunar module descent stage, a small proportion of probable natural seismic signals. The latter are long-duration, emergent oscillations which lack the discrete phases and coherence of earthquake signals. From similarity with the impact signal of the Apollo-12 ascent stage, they are thought to be produced by meteoroid impacts or shallow moonquakes. This signal character may imply transmission with high Q and intense wave scattering, conditions which are mutually exclusive on Earth. Natural background noise is very much smaller than on Earth, and lunar tectonism may be very low.

Latham, G. V., McDonald, W. G., and Moore, H. J.: 'Missile Impacts as Sources of Seismic Energy on the Moon', *Science* **168**, 242-246.

Seismic signals recorded from impacts of missiles at the White Sands Missile Range are radically different from the signal recorded from the Apollo-12 lunar module impact. This implies that lunar structure to depths of at least 10 to 20 kilometers is quite different from the typical structure of the Earth's crust. Results obtained from this study can be used to predict seismic wave amplitudes from future man-made lunar impacts. Seismic energy and crater dimensions from impacts are compared with measurements from chemical explosions.

Latham, G., Press, F., Toksoz, N., Wiggins, R., Sutton, G., Nakamura, Y., and Kovach, R.: 'Results from the Apollo Passive Seismic Experiment', *EOS* **51**, 363.

Data have been obtained from two lunar seismic stations established during Apollo missions 11 and 12. Of the many signals recorded, particularly by the Apollo-11 seismometers, most were generated by venting of gases from the lunar module descent stage. A small proportion of the signals are believed to be of natural origin. These signals are of long duration, with gradual buildup and decay, and do not show the distinct phases characteristic of earthquake signals. Natural signals are identified by their remarkable similarity to the signal recorded from the impact of the Apollo-12 lunar module ascent stage, and are thus thought to be caused by meteoroid impacts or shallow moonquakes. Expected meteoroid flux is sufficient to account for all of such observed signals. The signal character may imply transmission with a very high Q and intense wave scattering, conditions which are mutually exclusive on Earth. Natural background noise is much smaller than on Earth and lunar tectonism may be extremely low. (Abstract of a paper presented at the April 1970 meeting of the American Geophysical Union.)

Middlehurst, B. M. and Allen, N. C.: 'Operation LION: Report for Period of the Flight of Apollo-11', NASA-Contractor's Report-108476.

Naugle, J. E.: 'Announcement, Excerpts from NASA Description of Apollo-12 through 20', *Icarus* **12**, 134-139.

Candidate landing sites for Apollo-12 through 20 missions and experiments for the first five lunar landings are briefly described.

Sahinkaya, Y. E.: 'Minimum Energy Control of a Class of Electrical Driven Vehicles', NASA-Contractor's Report-109963; JPL-Technical Report-32-1471.

An automatic speed controller was designed and built for a class of electrically driven vehicles according to the theoretical concepts determined by the application of modern control theory. The theoretical and practical results given were originally aimed at the design and development of an automatic speed controller for lunar roving vehicles. For the vehicle considered, each wheel is driven by a permanent-magnet dc motor whose speed is governed by a controller with the following operational characteristics: (1) The controller accelerates or decelerates the vehicle to the desired speed in response to a command-signal fed into the system by the throttle mechanism in the presence of vehicle disturbances caused by terrain slope changes. (2) The controller maintains a constant vehicle speed at the desired value in the presence of terrain slope changes. (3) The controller accomplished the above by using a minimum amount of battery energy for the motor armature circuit during acceleration, and by feeding a maximum amount of energy from the motor armature circuit to the battery during deceleration.

Schneider, L. E.: 'Operation LION: Report for Network During Apollo-12', NASA-Contractor's Report-108477.

Spady, A. A. Jr.: 'Comments on Several Reduced-Gravity Simulators Used for Studying Lunar Self-Locomotive Tasks', NASA-Technical Note-D-5802.

The uncertainties concerning the physical capabilities and limitations of an explorer in performing locomotive and other working tasks in the lunar environment have led both industrial and governmental organizations to develop a variety of reduced-gravity simulators. This report presents a subjective review of the feel and operating characteristics of some of the simulators which are currently being used. The observations are those of an engineer who has acted as a test subject in a number of the currently developed simulators.

Spielberg, N. and Ziedins, G.: 'X-Ray Equipment for Lunar Receiving Laboratory' (Volume 1), NASA-Contractor's Report-108466.

A detailed description is presented of the design, fabrication, installation, and operation of an X-ray diffractometer and X-ray spectrograph system for preliminary examination of returned samples of lunar soil while these are still in quarantine within the Lunar Receiving Laboratory. The instrument heads are within the primary biological barrier at LRL and are operable by remote control from within the secondary biological barrier. The remote control may be accomplished by either a manual or computer control system. Emphasis is on the instruments and the manual control system.

Spielberg, N. and Ziedins, G.: 'X-Ray Equipment for Lunar Receiving Laboratory' (Volume 2, Part 1), NASA-Contractor's Report-108467.

Each instrument, the diffractometer and the spectrograph, employs an individual control system. Because of the similarity of both systems, a typical system applicable to either is described. Where special provisions are pertinent to one of the instruments, the exception is noted. Connector pin assignments for all connectors are given.

Swift, H. F., McGetchin, T. R., Preonas, D. D., and Johnson, S. W.: 'Laboratory Simulation of Apollo-12 Lunar Module Impact', *EOS* **51**, 347.

Plastic cylindrical caps and spheres were fired into unconsolidated targets at 4° and 5500 fps. High speed photography shows projectiles remained intact, contacted the surface for 8 to 10 projectile diameters, penetrated less than one diameter and skipped off at approximately the impact angle with

velocity reduced by about 10%. Craters were shallow, elliptical, commonly doublets. Ejecta was concentrated down range below about 30° and in two side lobes. Results suggest 80% of LM kinetic energy was delivered down range. LM and rock fragments could rain down near ALSEP from 40 sec to 3½ min after initial impact, an insufficient duration to account for the observed extended seismic signal; LM fragments may reimpact at 50 km past ALSEP at about 70 sec after initial impact. Seismic impulses may have been scattered in time and position. Landslides triggered by secondary impacts could produce an extended seismic signal although this idea is weakened by subsequent similar seismic events. The possible down range ballistic effects of objects purposely impacted at low angle and velocity may be significant and should be considered in future experiments. (Abstract of a paper presented at the April 1970 meeting of the American Geophysical Union.)

TRW Systems Group: 'Apollo Lunar Module Descent Engine Ablative Chamber: Injector Compatibility Improvement Study', NASA-Contractor's Report-1 082 170; TRW-11602-6090-R0-00.